Energy, Mines and Resources Canada
Earth Physics Branch
1 Observatory Crescent
Ottawa Canada
K1A 0Y3

Énergie, Mines et Ressources Canada
Direction de la physique du globe
1 Place de l'Observatoire
Ottawa Canada
K1A 0Y3

Geomagnetic Service of Canada

Service géomagnétique du Canada

AN INDUCTION ANOMALY NEAR THE WEST COAST OF HUDSON BAY, CANADA

by

J.C. Gupta, R.D. Kurtz and P.A. Camfield
Division of Seismology and Geomagnetism
Earth Physics Branch
Energy, Mines and Resources
Ottawa, Ontario
KIA 0Y3

EARTH PHYSICS BRANCH OPEN FILE NO. 83-29

pp. 55
Price/Prix: $11.00

Energy, Mines and Resources Canada
Énergie, Mines et Ressources Canada

Earth Physics Branch
Direction de la physique du globe

1 Observatory Crescent
Ottawa Canada
K1A 0Y3

1 Place de l'Observatoire
Ottawa Canada
K1A 0Y3

Geomagnetic Service of Canada

Service géomagnétique du Canada

AN INDUCTION ANOMALY NEAR THE WEST COAST OF HUDSON BAY, CANADA

by

J.C. Gupta, R.D. Kurtz and P.A. Camfield
Division of Seismology and Geomagnetism
Earth Physics Branch
Energy, Mines and Resources
Ottawa, Ontario
KIA OY3

EARTH PHYSICS BRANCH OPEN FILE NO. 83-29

pp. 55
Price/Prix: $11.00

TABLE OF CONTENTS

ABSTRACT

Geomagnetic data collected during the International Magnetospheric Study (IMS) are used to investigate the terrestrial electrical conductivity structure of northeastern Manitoba and part of the Northwest Territories. The computed transfer functions resolve a major east-west trending conductor between the communities of Gillam and Back in Manitoba. Regional trends in the surface geology suggest that this conductor might be linked with the North American Central Plains electrical conductor. Two-dimensional modelling of the data suggests that the conductor dips to the north from a shallow depth beneath Gillam and may extend to the lowermost crust.

RESUME

Les données géomagnétiques recueillies lors d'études internationales sur la magnétosphère (IMS) ont été utilisées afin d'investiguer la structure de la conductivité électrique de la terre pour le nord-est du Manitoba et une partie des Territoires du Nord-Ouest. La fonction de transfert calculée explique la présence d'un important conducteur orienté est-ouest, entre les villes de Gillam et Back au Manitoba. Les tendances régionales de la géologie de

surface suggèrent que ce conducteur soit relié avec celui des Plaines Centrales nord-américaines. Le modellage à deux dimensions, des données, suggère que le conducteur pend vers le nord, à partir d'une faible profondeur dans la région de Gillam, et peut se poursuivre jusqu'à la base de la croûte inférieure.

Introduction

In the magnetosphere, where incoming solar particles and energy are temporarily stored, complex energy transfers and interactions between plasmas, fields, waves and particles are continuously taking place. The influence of this space laboratory on the delicate balance of upper atmospheric dynamics and hence on weather systems and climate, on short wave radio propagation, on power transmission lines, etc., requires much study. Thus, the International Magnetospheric Study (IMS) project was proposed in the early 70's as a concerted effort to aquire ground based, balloon, rocket and satellite data to improve our understanding of the behaviour of the plasma environment of the Earth.

The Earth Physics Branch established an array of magnetometers along the Churchill magnetic meridian as part of the Canadian participation to IMS in order to study the ionospheric and magnetospheric current systems. The present investigation was undertaken to resolve any distortions of the ground magnetic observations by subsurface electric currents in the region of the Churchill array. The influence of the internal currents, if present, needs to be taken into account 1) to obtain meaningful ionospheric current models from the IMS data both during the quiet and magnetically disturbed times and 2) to help in the selection of appropriate sites for future magnetic observations for the CANOPUS (Canadian Auroral Network For The Open Program Unified Study) project of which magnetometer and riometer array (MARIA) is a significant element. The investigation involved calculation of transfer functions at all the stations.

DATA

Digital data at 10 s intervals were collected at the IMS magnetometer stations between September 1976 and June 1980. A detailed discussion of the data acquisition and of the derivation of average values at one minute intervals from the recorded 10 s data has been given by Plet and Jansen van Beek (1982). The description of the stations may be found in Table 1 and their locations are shown in Figure 1. The one minute data for Fort Churchill and Igloolik had been analysed previously by Dr. R.D. Kurtz (unpublished). The data used from Fort Churchill were for nine days in 1978 and from Igloolik for 12 days in 1981.

Fort Severn (FSV), (refer to Table 1 for the code names of other stations) had the fewest number of days with usable IMS data. Magnetograms of the data available from FSV were examined to select events with the intention of obtaining simultaneous records from the other stations of the Churchill Array. Thirty-five days at FSV were selected during which Z-variations were moderate ($\sum Kp \approx 23$) when compared with the observed general level of activity in this component and also in the H and D-components. Data simultaneously recorded with the selected FSV series were available for 11 of the 35 days from PEB, 26 days from RIT, 25 days from EKP, 26 days from BKC, 14 days from GIM, 28 days from TMP and 30 days from ISL. Information for FCC and IGL was taken from Kurtz's unpublished study.

For each day (00-24h UT), stacked plots of individual components H, D and Z for all stations allow a convenient inspection of the data. Some of these are shown in Figure 2 with the northernmost station at the top for each component.

All stations included in the study are strongly affected by auroral-zone and polar-cap currents. Large amplitude magnetic variations exist even under moderately disturbed conditions, as is seen in Figure 2a. The orientation of the source and its distance from the point of observation determine the variation in any component. Since these parameters change radically with time, variations may differ significantly from event to event. The stacked plots of a particular event may sometimes indicate the presence of additional currents flowing in an underlying conductor. Such indications may not be consistent from one event to another, however, because the internal contribution will depend on the frequency content and the polarization of the source field. Another important point is that the stations in the Churchill array, although on nearly the same geomagnetic meridian, are quite far apart from each other. Therefore, subjective inspections of the data will provide only a very general view of induction anomalies in the vicinity of the stations.

The influence of the external sources at these high latitudes is minimized by 1) careful selection of day-time events to eliminate the influence of the substorms and 2) taking time averages of the calculated transfer functions. Here, the assumption is that the external currents vary in position, sometimes drastically, but that the internal currents do not. So any effect left after averaging should be due primarily to the internal currents. Thus, for the present investigation the following criteria adopted by Handa and Camfield (1983) in the analysis of the Saskatchewan data have been closely followed:

1. Z-variations should have small amplitudes relative to the horizontal variations.

2. Day-time events are preferable. In the present case parts of magnetograms showing relatively low magnetic activity were generally taken.

3. Degree of polarization of the horizontal fields should be less than 0.7.

The variations shown in Figure 2a are typical of the data sets that have been used in the present investigation. Due to the compact form and the low sensitivity at which these plots are made, induction effects, especially at shorter periods, are not obvious. Figure 2b gives an expanded plot of the magnetic variations for 6 hours at some of the stations for September 4, 1979. Evidence for the existence of terrestrial conductors is difficult to discern from these figures, primarily from the disturbed character of the data. However, on the plot of the 10 s data in Figure 2c, which is an enlarged portion of Figure 2b, obvious large phase shifts or even reversals of the Z-component between BKC and GIM are observed. Such phase reversals of the Z-component are strong evidence of internal currents flowing between these two stations. Note that the influence of the longer duration substorms is quite clear at all stations and that at times, enhancement of the H-Component at BKC and GIM is recorded (e.g., Sept. 25, 1979 between 6-8h UT in Figure 2a). Sometimes the differences in the variation of the Z-component at BKC relative to other stations may also be seen on these plots. On May 11, 1977 between 6-8h UT a large phase difference or even a reversal in Z was noted at BKC and higher latitude stations, when compared to those stations to the south. Pulsational activity superimposed on the long period variations tends to have maximum amplitude at different stations during different events. These latter effects almost certainly are related to the locations of the external current sources.

Relative to H-component variations, those seen in the D-component are generally smaller for the majority of the events chosen. This implies that the relevant ionospheric source systems tend to flow east-west.

Following the criteria noted above, the available 12 hour intervals at each station were selected (in a few cases a smaller interval was taken) and average vertical-to-horizontal transfer functions were calculated following Edwards et al. (1971) and Bailey et al. (1974) at 22 different periods ranging from 122 sec to 30,720 sec (≃ 2 min - 512 min). A detailed discussion of the method of analysis is given in Appendix A.

The averaged values of the transfer functions are displayed in Figure 3 for all the stations. For each station the left and right side of the diagrams give respectively the amplitude and the azimuth of the real (in-phase) and imaginary (quadrature-phase) transfer functions. The azimuth represents the direction of horizontal variations which best correlate with the vertical variations; the amplitude gives the ratio of the vertical variations to these horizontal fluctuations. The error bars show the scatter amongst the averaged records and are one standard deviation from the mean values given by the circles for the real and the triangles for the imaginary transfer functions.

The plots in Figure 3 are included for completeness. The behaviour of the transfer functions is more easily visualized through the response arrow presentation in the next section.

Response Arrows

At periods 2.5, 4, 5, 10, 20, 40, 80, and 162 minutes, response arrows showing the relative amplitude and the direction of the transfer functions are displayed in Figure 4. Here the upper diagram gives the in-phase (real) and the lower diagram gives the quadrature phase (imaginary) response arrows. The arrows for the in-phase transfer functions have been reversed in direction so as to point towards the internal currents and away from the external currents.

In general, the in-phase arrows at PEB and IGL have large amplitudes and point north-west. Those at RIT and EKP have smaller amplitudes and point south-east for periods of up to 10 minutes. Such a situation may arise if uniform external currents are flowing closer to PEB and IGL but are far away from the rest of the stations (Loomer and Gupta, 1980). This partially satisfies the condition that vertical variations due to the external sources, at the stations of interest for induction investigations, are very small (condition 2). However, magnetic variations at PEB and IGL would also be influenced by electric currents flowing in the conducting salt water bodies to the north.

A systematic change is noted in the direction of the in-phase arrow at PEB from 20 minutes period to 162 minutes period; this change in direction can also be seen in Figure 3. At 80 minutes period the PEB in-phase arrow points south-west while RIT and EKP arrows point almost in the opposite direction to the north-east. At both shorter and longer periods the PEB arrow is not antiparallel to those at RIT and EKP. Based on the oppositely directed arrows one may speculate the presence of a thin east-west elongated conductor,

between PEB and the RIT/EKP pair of stations, buried in the upper mantle of the earth to which depth waves with periods of nearly 80 minutes penetrate. Alternatively, a polar jet (Loomer and Gupta, 1980) flowing between PEB and IGL and an auroral electrojet flowing between EKP and FCC may cause the observed orientation of the in-phase arrows at 80 minutes period.

Figure 4 shows that the in-phase arrows at GIM point northwards and at BKC southwards. The arrows to the west of GIM at TMP and to the east at FSV closely follow the direction of the arrow at GIM up to a period of about 80 minutes. On the other hand, arrows at FCC, EKP and RIT follow the direction of the arrow at BKC at least up to a period of 10 minutes. At longer periods the observed directions of the arrows at FCC, EKP and RIT are most probably influenced by the auroral electrojet currents. At short periods the azimuth angles at ISL, TMP, GIM, FSV, BKC and FCC are reasonably well defined and the oppositely directed arrows seem to be related to phase reversals in the Z-component between BKC and GIM as shown in Figure 2c. These observations are probably related to anomalous internal currents that flow in an internal electrical conductor that passes east-west from north of TMP, goes between BKC and GIM, and most likely also passes to the north of FSV. From skin depth considerations one would expect the conductor to be a body with the lower edge sufficiently deep in the earth to affect induction arrows of periods up to 80 minutes and more.

North-South Profiles

The north-south component of the transfer function amplitude was calculated using the equation -

$$L_{Re,Qu} = \ell_{Re,Qu} \cos (\theta_{Re,Qu} + D^\circ)$$

where $\ell_{Re,Qu}$ is the amplitude of the Real (Quadrature) transfer function and $\theta_{Re,Qu}$ lie between $\pm 180°$ and are the angles made by the induction arrows with the local geomagnetic meridian (see equation 25 in Appendix A), and D° is the declination at a station. The north-south profiles given in Figure 5 are drawn using the calculated values of L.

Except for FSV the latitudinal profiles of the transfer function amplitudes are quite smooth and similar at all periods. Any changes are gradual from short to long periods. In general form the profiles represent the vertical magnetic field (normalized by the horizontal field) which would arise from east-west currents flowing within the earth between the latitudes of BKC and GIM/FSV.

FSV is east of the main north-south line of stations and may be affected by the currents flowing in the saline water of Hudson Bay. This is supported by the eastward tendency of the induction arrows at RIT, EKP and FCC. These currents may enhance the amplitude of the FSV real transfer function at short periods (2.5-5 minutes) and that of the quadrature transfer function at periods from 2.5-20 minutes. Our estimate of the distortions of the amplitude profiles at FSV are shown by the dotted lines in Figure 5. At longer periods from 10 minutes to 162 minutes the amplitude of the real transfer function is lower than at GIM and TMP, as is the quadrature transfer function from periods of about 40 to 162 minutes. The currents flowing in the saline water of Hudson Bay may be expected to aid the internal currents flowing in a conductor buried in the crust. The reduction in the amplitude of the transfer functions at the long periods suggests that the conductor may only extend to shallower depths at this location.

Conductive Structure

To study the structure of the internal conductor evident in the transfer functions, the E - polarization response of a two-dimensional inhomogeneous earth was calculated, following Ku et al. (1973). For the model calculations it was assumed that a conductor (resistivity = 25 ohm.m) lies within a resistive crust and upper mantle (5000 ohm.m) that extends to a depth of about 130 km. Underneath is a conducting basement (200 ohm.m). For the model of the area under consideration, high crustal resistivities have been assumed, similar to those reported elsewhere in the Canadian Shield (Strangway et al., 1980). The computed transfer functions obtained from the ratio of the vertical to the horizontal fields at periods of 2.5 minutes and at 20 minutes were compared to the profiles described in Figure 5, which were considered to be transverse to the strike of the east-west conductor. Various models were computed, i.e., conducting bodies with rectangular cross-section and several widths and depths, conductors dipping towards higher or lower latitudes, etc. The model that provides the best fit to the observed real and quadrature transfer functions at both the short (2.5 min) and long (20 min) periods is shown in Figure 6 and is henceforth called the "selected model". Results of some experiments, in which parameters of the host medium and of the conductor such as its width, depth, conductivity, etc. were varied, are given in Table 2. The model transfer functions are graded A, B or C for decreasing quality of fit to the measured transfer functions on the north-south profiles. The selected model is the reference with uniform A grades.

It is obvious from the tables that the fit remains unchanged whether the conductor comes to the surface of the Earth or is buried 5 km deep. A narrower conductor improves the fit to the short period profiles but some

deterioration is noted in the fit of the long period in-phase transfer functions. On the other hand, a wider conductor improves the fit to the real transfer function amplitude profile at long periods but the fit deteriorates for shorter periods and so on. Based on the information given in Table 2, the following may be said with some degree of certainty about the conductor on the western coast of Hudson Bay:

1) The conductor influences the observations at BKC and GIM most, to give oppositely-directed response arrows at these two stations. TMP and FSV are also strongly influenced.

2) It is buried in an environment of high resistivity (≥2500 ohm.m). There was little change in the quality of fit when the resistivity was lowered to 2500 ohm.m or raised to 25,000 ohm.m.

3) The lateral position of the top of the conductor is constrained reasonably well between GIM and BKC, but is closer to GIM than BKC.

4) The depth to the top of the conductor is not well constrained by the data and could be as great as 10 km. The conductor may extend to the bottom or below the base of the earth's crust at a depth of about 40 km (Innes et al., 1972).

5) The top of the conductor appears to be about 40 km wide with the southern end under GIM or possibly slightly south of GIM. The body gradually becomes wider at greater depths and may be 60-80 km wide near its greatest depth. It dips towards higher latitudes.

6) Its resistivity lies between 10-50 ohm.m with the best fit to the observed data being achieved for a value of 25 ohm.m.

Despite the above, it needs to be emphasized that the selected model cannot be considered unique. It is only one of many other possibilities that may produce similar or better results.

GEOLOGICAL AND TECTONIC IMPLICATIONS

Recently, Lewry (1981), Lewry et al. (1981) and Green et al. (1983) have summarized the known geological features of the Saskatchewan-Manitoba area. It may be seen from Figure 7 (from Green et al. 1983) that the area has been subdivided into several tectonic/geologic zones. The conductor is in the vicinity of the easterly extensions of the Wollaston-Chipewyan batholith and the La Ronge-Lynn Lake, Reindeer-South Indian Lakes and Kisseynew belts. North and west of these terrains lies the Cree Lake zone (Wollaston and Seal River domains) and to the south lies the Glennie Lake domain, the Tabbernor fault/fold zone and the Flin Flon-Snow Lake, Thompson and Fox River belts. According to Green et al. the La Ronge-Lynn Lake and Flin Flon-Snow Lake belts are granite/greenstone terrains of Proterozoic age and are composed of volcanic island-arc assemblages. The geology is poorly known because of lack of exposure in the vicinity of the stations. The Wathaman-Chipewyan batholith is a composite of granite to monzonitic to granodioritic intrusive rocks and is exposed for a length exceeding 800 km between the cover rocks of the Williston and Hudson Bay basins. Rocks in the Kisseynew and Reindeer-South Indian Lakes belt are mainly greywackes, siltstones and mudstones that have been subjected to high grades of metamorphism to form paragneisses, migmatites and in the central regions of the belt anatectic granitic bodies. These rocks

originated as volcanic detritus from the nearby volcanic island arcs transported in part by turbidity currents.

The Gillam-Back conductor found in this study runs east-west and appears to have its southern edge beneath GIM or slightly to the south and extends northwards 60-80 km towards BKC (distance between BKC and GIM is about 145 km). This suggests that the conductor lies beneath geological units identified tentatively as cordillerian-type arc massifs and highly reworked oceanic material (former fore-arc or back-arc basins north of the Fox River belt).

Handa and Camfield (1983) have shown that the North American Central Plains (NACP) conductivity anomaly extends into Saskatchewan where it lies beneath the Rottenstone-La Ronge magmatic belt. This belt in Figure 7 consists of the Wathaman-Chipewyan batholith, the Reindeer-South Indian Lakes and La Ronge-Lynn Lake belts. However, the Gillam-Back conductor relates most closely to the surface exposure of the Kisseynew belt rocks, whereas the NACP is related to the more northerly structures. It is likely however that it passes beneath the Reindeer-South Indian belt, and/or the La Ronge-Lynn Lake belt as shown in Figure 8 and also by Green et al. (1983).

Both the NACP conductor in Saskatchewan and the Gillam-Back conductor in Manitoba on the west coast of Hudson Bay are major structures. The geological trends suggest that the NE-SW structure in Saskatchewan turns E-W in Manitoba. In general terms this is the basis for speculations that the NACP structure links with the Gillam-Back structure. In detail it is hard to correlate this claim with surface geology, since the station spacing is too

sparce in both areas, especially in Manitoba. Figure 8 shows the NACP conductor and a possible link with the Manitoba part of the Gillam-Back conductor.

The transfer function results at FSV suggest an extension of the Gillam-Back conductor eastwards under Hudson Bay. The tectonic or geological processes that caused the electrical conductors which appear to satisfy the observations of Handa and Camfield (1983) and of the present study are not clear. Handa and Camfield suggested that conductive mineralization or the presence of saline water in fractured rocks may have lead to the production of conductive bodies. In this connection Camfield and Gough (1977) have noted that "there are salt solution features in the Devonian Prairie evaporite formation which lie along the trend of the conductor in southern Saskatchewan. Faults in the basement might have influenced the removal of the salt; the high electrical conductivity could be caused by saline water in the fractures". On the other hand, the possible association of the conductor with ancient former oceanic crust may indicate that the high conductivity arises from conductive mineralization related to partial serpentinization of ocean basalt at a ridge crest (de Beer et al., 1982).

ACKNOWLEDGEMENTS

We are very grateful to Mr. Fred C. Plet of the Earth Physics Branch for providing us with the edited IMS data used in this study. We also thank Dr. A.G. Green for valuable discussions especially on the geology of the area and also for the permission to use material from the preprint of his paper. The assistance and guidance in the preparation of the manuscript provided by Dr. E.R. Niblett is very much appreciated.

APPENDIX A

Geomagnetic Depth Sounding Method and Transfer Functions

A technique commonly known as "Geomagnetic Depth Sounding" (GDS) is employed to study the conductivity structure of the crust and mantle of the earth. In this method, natural variations in the three geomagnetic components are recorded simultaneously at a number of stations appropriately located in the region of investigation. The electric currents induced in the underlying conductors influence the variation of the geomagnetic components measured at these stations. Thus a study of the differences in the amplitudes and phases of these components as a function of frequency can indicate the existence of anomalous conductivity structures. Some of these conductors are located in areas of high heat flow and low seismic velocity.

Magnetic storms and substorms whose currents mainly flow in the ionosphere and magnetosphere at the auroral latitudes provide the best sources for GDS experiments at mid and low latitudes. This is because the return currents associated with these far-off sources are quite spatially uniform at these latitudes. Therefore any sharp local changes in amplitude and phase at adjacent stations can be reasonably well ascribed to the underlying inhomogeneous conductivity structure which influences the induced currents. In a homogeneous or layered medium the induced currents give rise to a normal internal vertical field which is in the opposite direction of the external vertical component of the incident variation field. This leads to an overall suppression of the normal vertical field variation. On the other hand, the normal internal horizontal fields lead to an enhancement of the normal

horizontal components of the external incident variation field by virtue of their being in the same direction. Thus a suppressed vertical component variation and an enhanced horizontal component variation are good indications of the presence of a conductor underneath the array of stations.

Because of the concentration of electric currents in a conductor relative to its surroundings, the component of the horizontal field perpendicular to the strike of the conductor produces an anomalous internal vertical field which is in addition to the normal internal vertical field mentioned above. This anomalous vertical field is therefore correlated with an external horizontal field when its variations (i.e. the variations of the external horizontal field) are in a particular direction. If the external current sources are nearly uniform over a lateral conducting structure, the normal Z-component variations are small and the anomalous part constitutes a greater portion of the recorded vertical component than the contribution of the anomalous part to either of the horizontal components. As mentioned above this usually is the case at mid and low latitude stations. On the other hand magnetograms of disturbed times from high latitude stations sometimes do not reveal the influence of the currents flowing into the subsurface conductors presumably because the source field effects overwhelm those of the conductor. Anomalous fields may also arise due to large scale electric current systems flowing near the coast of a large ocean.

Through his pioneering induction studies, Parkinson (1959, 1962, 1964) defined an arrow which came to be known as Parkinson's vector, that points towards the region of enhanced conductivity, such that the arrow indicates the horizontal direction (ϕ) in which the upwards (negative Z) vertical change

has maximum correlation with the horizontal field changes. The length of the arrow (R) is given by the ratio of the vertical to the horizontal variations. If H, D and Z are respectively the horizontal intensity, eastward declination and downward vertical intensity and ΔH, ΔD and ΔZ are their fluctuations (during a magnetic storm or substorm) at equal intervals (say 20 minutes) then -

$$\phi = \tan^{-1} \frac{A \cdot \Delta D}{\Delta H}; \qquad \theta = \tan^{-1} \frac{((\Delta H)^2 + (A \cdot \Delta D)^2)^{1/2}}{\Delta Z}$$

$$\text{and } R = \frac{\Delta Z}{((\Delta H)^2 + (A.\Delta D)^2)^{1/2}} \qquad \text{where } A = \frac{H}{3440}$$

Here ΔH and ΔZ are expressed in nT, D in minutes of arc (1 minute of arc = 1/3440 radians) and H is the average horizontal intensity. Let us denote the vector variation of the magnetic field by OP at a given location. Then θ (angle of tilt) is the angle made by the vector OP with the upward vertical. Similarly ϕ is the angle made by the

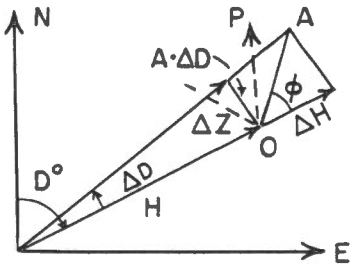

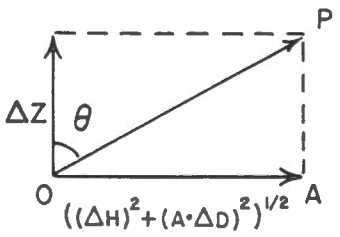

$$OP = ((\Delta H)^2 + (A \cdot \Delta D)^2 + (\Delta Z)^2)^{1/2}$$

$$OA = ((\Delta H)^2 + (A \cdot \Delta D)^2)^{1/2}$$

horizontal projection of OP with magnetic north (The horizontal projection of OP is in the direction of OA). The vector OP points in the direction of the preferred plane.

Several events and intervals must be analysed to accurately obtain the above parameters for a site.

Some evidence of the presence and influence of the subsurface structures at individual stations is obtained by calculating the transfer functions from

the geomagnetic data of moderate amplitude storms or substorms. Briefly the transfer functions, which are analogous to the Parkinson's vector, are discussed below following Schmucker (1970) and Bailey et. al (1974).

Suppose H(t) and Z(t) are two linearly related functions normalised to zero mean in the interval $-\frac{T_o}{2} \leq t \leq \frac{T_o}{2}$ where $T_o \to \infty$. Their relations being independent of time in this interval, they can be expressed by a transfer function $z_H(f)$ in the frequency domain. In terms of the Fourier Transforms H(f) and Z(f) we can write.

$$\begin{pmatrix} H(f) \\ Z(f) \end{pmatrix} = \int_{-\infty}^{\infty} \begin{pmatrix} H(t) \\ Z(t) \end{pmatrix} e^{-2\pi i f t} \, dt \tag{1}$$

and

$$Z(f) = z_H(f) \cdot H(f) \tag{2}$$

where $z_H(f)$ is the transfer function which can be written as $z_H(u)+iz_H(v)$ (Schmucker, 1970). The amplitude of the transfer function is $((z_H^2(u) + z_H^2(v))^{1/2}$ and the phase lead of Z(t) relative to H(t) is

$$\arctan \frac{z_H(v)}{z_H(u)}.$$

The product of H(f) with its complex conjugate H*(f) is called the power spectrum S_{HH} of H(t) and similarly the product of Z(f) with H*(f) is called the cross spectrum S_{ZH} between Z(t) and H(t). Thus

$$S_{HH} = H(f) \cdot H^*(f) \text{ and } S_{ZZ} = Z(f) \cdot Z^*(f) \tag{3}$$

and

$$S_{ZH} = Z(f) \cdot H^*(f) = S_{HZ}^*. \tag{4}$$

Then equation (2) gives -

$$z_H(f) = \frac{Z(f)}{H(f)} = \frac{S_{ZH}}{S_{HH}} \tag{5}$$

which expresses the transfer function in terms of the power and cross spectra.

Coherence and Residual

Let $\delta Z(t)$ be the uncorrelated noise in $Z(t)$ whose correlated power $|Z(f)|^2$ is given by equation (2). The power of the noise therefore is

$$S_{\delta Z} = S_{ZZ} - (z_H(f) \cdot H(f))\ (z_H^*(f) \cdot H^*(f))$$

and by equation (5) this gives

$$S_{\delta Z} = S_{ZZ} - \frac{|S_{ZH}|^2}{|S_{HH}|^2} \times S_{HH}$$

$$= S_{ZZ} - \frac{|S_{ZH}|^2}{S_{HH}} \quad . \tag{6}$$

The square root of the normalised correlated power is known as coherence $C_o(f)$ and the square root of the normalised uncorrelated power is known as residual $E_o(f)$. Thus-

$$C_o(f) = \left(\frac{S_{ZZ} - S_{\delta Z}}{S_{ZZ}} \right)^{1/2} \quad \text{and} \quad E_o(f) = \left(\frac{S_{\delta Z}}{S_{ZZ}} \right)^{1/2} \tag{7}$$

These give-

$$C_o^2(f) = 1 - E_o^2(f)$$

and in view of equation (6)

$$C_o^2(f) = \frac{|S_{ZH}|^2}{S_{ZZ} \cdot S_{HH}} \quad . \tag{8}$$

$C_o(f)$ varies between zero in the case of no correlation at a certain frequency and unity in the case of a one-to-one correlation. Also if ν denotes the degree of freedom of the analysis then a value of $C_o(f) \geq \left(\frac{4}{\nu}\right)^{1/2}$ implies a significant dependence between the two time series. Usually the spectra appearing in equation 5 are determined by averaging the spectra of K isolated events. Thus K=1 event would determine the transfer function $z_H(f)$ uniquely with zero residuals, i.e., with zero degree of freedom. Each

additional event adds two degrees of freedom because for each event the Fourier Transform has a real (cosine) and an imaginary (sine) part. Hence the degree of freedom $\nu = 2(K-1)$.

Let $H_a(t)$, $D_a(t)$ and $Z_a(t)$ represent the anomalous part of the north H(t), east D(t) and vertically downward Z(t) components of the geomagnetic variations during a particular event measured at a site in a region of anomalous conductivity. Also let $H_N(t)$, $D_N(t)$ and $Z_N(t)$ be the components of the normal geomagnetic variations at the same site that would have been measured had the conducting anomaly been absent. Sometimes the normal variation components are obtained from a station located outside the anomalous region.

Based on the earlier discussion a matrix of transfer functions relating the anomalous and the normal variations in the frequency domain may now be written as follows:

$$\begin{pmatrix} H_a(f) \\ D_a(f) \\ Z_a(f) \end{pmatrix} = \begin{pmatrix} h_H & h_D & h_Z \\ d_H & d_D & d_Z \\ z_H & z_D & z_Z \end{pmatrix} \begin{pmatrix} H_N(f) \\ D_N(f) \\ Z_N(f) \end{pmatrix} + \begin{pmatrix} \delta H(f) \\ \delta D(f) \\ \delta Z(f) \end{pmatrix} \qquad (9)$$

$H_a(f)$, $H_N(f)$ and $\delta H(f)$ are Fourier Transforms of $H_a(t)$ $H_N(t)$ and $\delta H(t)$ and so on. The 3 x 3 matrix contains transfer functions between the anomalous and the normal fields. The right-hand 3 x 1 matrix represents the portion of the anomalous field uncorrelated with the normal field. The matrix of the transfer functions needs to be determined in such a way that the uncorrelated power in the observed variations H(t), D(t) and Z(t), namely $\delta H(f)$. $\delta H^*(f)$, etc. must be a minimum, for each resolved frequency component when averaged over a frequency interval or a sequence of events.

According to Banks (1973) "A practical definition of a normal station is that it should be one situated above a horizontally stratified conductivity structure and sufficiently distant from any lateral discontinuities as to be unaffected by the associated anomalous internal currents". Also at such a station "....when the spectral estimates are averaged over sufficient quantities of data, the coherence between any pair of components H,D and Z should be zero". Further, spatial changes in the source field may influence the survey site and the normal station differently. Because of these considerations, and especially because of the difficulty of finding a normal station, a single-station transfer function analysis is usually carried out. In this method of analysis the transfer functions in the upper two rows of the 3 x 3 matrix given by equation (9), which enter in the equations for $H_a(f)$ and $D_a(f)$, cannot be estimated accurately (Banks, 1973). However the anomalous part in the observed vertical field variations is given by

$$Z_a(f) = z_H H_N(f) + z_D D_N(f) + z_Z Z_N(f) + \delta Z(f) \qquad (10)$$

In order that the residual uncorrelated power $S_{\delta Z}=\delta Z(f)\cdot\delta Z^*(f)$ is a minimum, the following first derivatives must be set to zero:

$$\frac{\partial S_{\delta Z}}{\partial z_H(u)}, \frac{\partial S_{\delta Z}}{\partial z_H(v)}, \frac{\partial S_{\delta Z}}{\partial z_D(u)}, \frac{\partial S_{\delta Z}}{\partial z_D(v)}, \frac{\partial S_{\delta Z}}{\partial z_Z(u)}, \text{and } \frac{\partial S_{\delta Z}}{\partial z_Z(v)}.$$

In view of equation (10)

$$S_{\delta Z} = (Z_a(f) - (z_H H_N(f) + z_D D_N(f) + z_Z Z_N(f)))\,(Z_a^*(f) - (z_H^* H_N^*(f) + z_D^* D_N^*(f) + z_Z^* Z_N^*(f)))$$

Recall that $z_H = z_H(u) + iz_H(v)$ and $z_H^* = z_H(u) - iz_H(v)$ etc. Then on taking the partial derivatives:

$$\frac{\partial S_{\delta Z}}{\partial z_H(u)} = -Z_a(f)H_N^*(f) - H_N(f)Z_a^*(f) + H_N(f)z_H^*H_N^*(f) + z_H H_N(f)H_N^*(f)$$
$$+ H_N(f)z_D^*D_N^*(f) + H_N(f)z_Z^*Z_N^*(f) + z_D D_N(f)H_N^*(f) + z_Z Z_N(f)H_N^*(f)$$

$$= - H_N^*(f)\ (Z_a(f) - (z_H H_N(f) + z_D D_N(f) + z_Z D_N(f)))$$

$$- H_N(f)\ (Z_a^*(f) - (z_H^* H_N^*(f) + z_D^* D_N^*(f) + z_Z^* Z_N^*(f))),$$

$$= - H_N^*(f)\ \delta Z(f) - H_N(f)\ \delta Z^*(f) \equiv 0$$

$$\text{or} \qquad \delta Z(f) \cdot H_N^*(f) = -\delta Z^*(f) \cdot H_N(f). \tag{11}$$

Similarly

$$\frac{\partial S_{\delta Z}}{\partial z_H(v)} = i\{H_N^*(f)\ \delta Z(f) - H_N(f)\ \delta Z^*(f)\} \equiv 0$$

$$\text{or} \qquad \delta Z(f) \cdot H_N^*(f) = H_N(f) \cdot \delta Z^*(f). \tag{12}$$

Since $\delta Z(f) \cdot H_N^*(f)$ is purely imaginary in view of equation (11) and purely real in view of equation (12), it is concluded that -

$$\delta Z(f) \cdot H_N^*(f) \equiv 0 \tag{13}$$

Also by calculating $\frac{\partial S_{\delta Z}}{\partial z_D(u)}$, $\frac{\partial S_{\delta Z}}{\partial z_D(v)}$, $\frac{\partial S_{\delta Z}}{\partial z_Z(u)}$ and $\frac{\partial S_{\delta Z}}{\partial z_Z(v)}$

it may be seen that

$$\delta Z(f) \cdot D_N^*(f) \equiv 0 \tag{14}$$

$$\text{and} \qquad \delta Z(f) \cdot Z_N^*(f) \equiv 0. \tag{15}$$

Therefore the minimum condition requires that the cross spectra between the uncorrelated part δZ and the normal parts ($H_N(f)$, $D_N(f)$ and $Z_N(f)$ are zeros i.e.

$$S_{\delta Z H_N}(f) \equiv S_{\delta Z D_N}(f) \equiv S_{\delta Z Z_N}(f) \equiv 0. \tag{16}$$

If equation (10) is multiplied by $H_N^*(f)$, $D_N^*(f)$ and $Z_N^*(f)$ and averaged over a large number of records (averages to be denoted by $\{\}$) and if the conditions given in equations 13-15 are used, the following equations are obtained

$$\{H_N^*(f)Z_a(f)\} = z_H\ \{H_N^*(f)H_N(f)\} + z_D\ \{H_N^*(f)D_N(f)\} + z_Z\ \{H_N^*(f)Z_N(f)\}$$

$$\{D_N^*(f)Z_a(f)\} = z_H\ \{D_N^*(f)H_N(f)\} + z_D\ \{D_N^*(f)D_N(f)\} + z_Z\ \{D_N^*(f)Z_N(f)\} \tag{17}$$

$$\{Z_N^*(f)Z_a(f)\} = z_H\ \{Z_N^*(f)H_N(f)\} + z_D\ \{Z_N^*(f)D_N(f)\} + z_Z\ \{Z_N^*(f)Z_N(f)\}.$$

At any station the vertical anomalous field of an event could be defined as the difference of the observed field Z(t) and the normal field $Z_N(t)$ at a station outside the anomalous region. In terms of the Fourier Transforms we can write

$$Z_a(f) = Z(f) - Z_N(f). \tag{18}$$

It has been mentioned earlier that a systematic difference may exist in the source field, due to its spatial variations, at the field station and at the normal station and that also it is difficult to find a normal station. Thus equations (17) are solved by making the following assumptions in the single station technique-

1) On the average, the normal part of vertical variations have negligible correlation with the normal parts of the two horizontal components. This implies that -

$$\{Z_N(f)H_N^*(f)\} = \{Z_N(f)D_N^*(f)\} = 0 \tag{19}$$

and equation (18) then gives -

$$\{Z_a(f)H_N^*(f)\} = \{Z(f)H_N^*(f)\}$$

$$\{Z_a(f)D_N^*(f)\} = \{Z(f)D_N^*(f)\}. \tag{20}$$

That is, the cross spectra between the anomalous vertical and the normal horizontal components are equivalent to the cross spectra between the observed vertical component and the normal horizontal components.

2) The normal part of vertical variations have negligible correlation with the anomalous part of vertical variations (The validity of this assumption rests on the fact that at mid latitude stations, vertical variations are much smaller than horizontal variations over a horizontally stratified earth). This implies -

$$\{Z_N^*(f)\ Z_a(f)\} = 0 \tag{21}$$

i.e. the 3rd part of equation (17) vanishes. The applications of equations (19), (20) and (21) to equation (17) then gives -

$$\{H_N^*(f)Z(f)\} = z_H \{H_N^*(f)\, H_N(f)\} + z_D \{H_N^*(f)\, D_N(f)\}$$

$$\{D_N^*(f)Z(f)\} = z_H \{D_N^*(f)\, H_N(f)\} + z_D \{D_N^*(f)\, D_N(f)\}.$$

These equations are solved easily to give the transfer functions $z_H(f)$ and $z_D(f)$ at a fequency (f) -

$$z_H(f) = \frac{\{H_N^*(f)Z(f)\}\{D_N^*(f)D_N(f)\} - \{D_N^*(f)Z(f)\}\{H_N^*(f)D_N(f)\}}{\{H_N^*(f)H_N(f)\}\{D_N^*(f)D_N(f)\} - \{D_N^*(f)H_N(f)\}\{H_N^*(f)D_N(f)\}}$$

$$z_D(f) = \frac{\{D_N^*(f)Z(f)\}\{H_N^*(f)H_N(f)\} - \{H_N^*(f)Z(f)\}\{D_N^*(f)H_N(f)\}}{\{H_N^*(f)H_N(f)\}\{D_N^*(f)D_N(f)\} - \{D_N^*(f)H_N(f)\}\{H_N^*(f)D_N(f)\}} \qquad (22)$$

and the transfer function $z_Z(f)$ is zero.

3) finally, remote from conductivity structures one can safely substitute H and D for H_N and D_N implying also that the anomalous field variations are mainly confined to the vertical component i.e., the horizontal fields from internal currents are small with respect to the source fields. Now, in terms of the auto and cross power spectrum the transfer functions can be written as -

$$z_H(f) = \frac{S_{ZH}\, S_{DD} - S_{ZD}\, S_{DH}}{S_{HH}\, S_{DD} - |S_{HD}|^2}$$

$$z_D(f) = \frac{S_{ZD}\, S_{HH} - S_{ZH}\, S_{HD}}{S_{HH}\, S_{DD} - |S_{HD}|^2}. \qquad (23)$$

Since $z_H(f)$ and $z_D(f)$ are complex numbers they can be represented in the form of real and quadrature induction arrows (IA). The directon of the real IA is usually reversed so that it corresponds to Parkinson's vector and points towards the conductivity structure. Thus -

$$z_H = z_H(u) + i\, z_H(v)$$

$$z_D = z_D(u) + i\, z_D(v)$$

and

$$\text{Re IA} = -z_H(u)\, \hat{i} - z_D(u)\hat{j}$$

$$\text{Qu IA} = z_H(v)\, \hat{i} + z_D(v)\hat{j}$$

where $\hat{i}$ and $\hat{j}$ are unit vectors in the H and D directions. At a specific frequency the magnitudes of the real and quadrature IA's are then-

$$M_{Re} = (z_H^2(u) + z_D^2(u))^{1/2} \quad \text{and} \quad M_{Qu} = (z_H^2(v) + z_D^2(v))^{1/2} \qquad (24)$$

and the angles made by the IA with the local geomagnetic meridian are -

$$\theta_{Re} = \tan^{-1} \frac{z_D(u)}{z_H(u)} \quad \text{and} \quad \theta_{Qu} = \tan^{-1} \frac{z_D(v)}{z_H(v)} \qquad (25)$$

and are measured in a clockwise or eastward direction from the meridian and vary between -180° to +180°.

The in-phase IA's point towards zones of high internal conductivity. According to Edwards et. al (1971) if the correlated vertical and horizontal components are produced by channelled currents or if the internal induced field is in-phase with the external inducing field, the vectors are purely real. Quadrature IA's only arise when there is phase shift between the

external and internal fields. They are usually caused by near-surface conductivity anomalies as the superficial eddy currents have a large phase lead relative to the inducing field. Hence the secondary field resulting from these eddy currents would also have a large phase lead.

As noted in the previous section, in the present case at least two events are necessary to determine the transfer functions $Z_H(f)$ and $Z_D(f)$ uniquely with zero residuals. Therefore when K isolated events are used to determine the transfer functions $z_H(f)$ and $z_D(f)$ the degree of freedom is $\nu = 2\ (K-2)$ and for a meaningful coherence at a particular frequency the permissible upper limit of the residual is given by

$$\left(1-\frac{4}{\nu}\right)^{1/2} = ((K-4)/(K-2))^{1/2}.$$

A brief discussion of the treatment of the IMS data that were used for analysis follows.

Let us consider a digitized quasi-stationary time series X" with total number of data points N':

$$X"_r = x_r \text{ where } r = 1, 2, 3 \ldots N'. \tag{26}$$

When the mean of such a series is not zero a large peak (theoretically infinite) appears in the spectrum at the zero frequency which distorts estimates of power at adjacent frequencies. Therefore the mean given by the following equation is first removed from the time series -

$$\bar{X} = \frac{1}{N'} \sum_{r=1}^{N'} x_r. \tag{27}$$

In the present analysis shorter period (≦3 hours) variations are of interest. Therefore the linear trends in the data caused by long period changes such as diurnal variation of the magnetic field, instrument drift etc., that tend to distort the calculated spectra at higher frequencies, need to be removed. This is done by the method of Bendat and Piersol (1966) who defined the average slope of a time series by the equation -

$$\bar{a} = \frac{1}{L(N'-L)}\left(\sum_{j=N'-L}^{N'} x_j - \sum_{j=1}^{L} x_j\right) \tag{28}$$

where L is the largest integer less than or equal to N'/3. When this slope is linearly subtracted along with the mean given by equation (27) a new time series with zero mean and zero average slope results, i.e.

$$X'_r = x_r - \bar{X} - \bar{a}\,(r - \frac{N'}{2}). \tag{29}$$

In Fourier analysis it is assumed that a digitized time series of length T is periodic with a fundamental period T. When sudden changes, leading to differing amplitudes at the beginning and at the end of the time series are present, high frequency components are introduced to the spectrum which tend to alter the true spectrum. These kinds of discontinuities are reduced by tapering the first and last 10% of the time series to zero by using a quarter sine wave. Because the first and the last quarter of the wave are separated by a long straight line, the resulting curve looks like a cosine wave and hence this special filter is known as a cosine taper. Thus for the new time series X_r the first and last 10% of the data given by equation (29) become respectively -

$$x_j = x_j \sin\left(\frac{\pi}{2}\,\frac{(j-1)}{(R-1)}\right)$$

and

$$x_k = x_k \sin\left(\frac{\pi}{2}\frac{(j-1)}{(R-1)}\right) \tag{30}$$

where $j = 1, 2, 3, \ldots\ldots\ldots\ldots R-1$

$k = N' - (j-1)$

and R denotes 10% of the total number of data points i.e. $\frac{N'}{10}$.

The Fast Fourier Transform (FFT) technique developed by Cooley and Tukey (1965) is then applied to the reconditioned time series (30) to obtain spectra. In this method it is necessary to add zeros at the end of the series as the Cooley-Tukey algorithm requires the number of data points to be a power of 2. In our case the minute values of 12 hours provided 720 points to which 304 zeros were added at the end to make the series $1024(=2^{10})$ points long. According to Gold and Rader (1969) this also eliminates distortion of the covariences by the periodic covariences. Thus the total number of points in the series becomes -

$$N = N' + \text{number of zeros} \tag{31}$$

The discrete Fourier Transform of a time series X_n sampled at N equally spaced intervals (Δ) of time for the duration T is given by the equation-

$$\begin{aligned} X_k(w) &= \sum_{n=0}^{N-1} x_n e^{-i\left(\frac{2\pi k}{N\Delta}\right)\Delta n} \\ &= \sum_{n=0}^{N-1} x_n e^{-2\pi i\left(\frac{kn}{N}\right)} \end{aligned} \tag{32}$$

with the Fourier Coefficients given at frequencies-

$$w = \frac{2\pi k}{N\Delta} = \frac{2\pi k}{T} \qquad k = 0, 1, 2, \ldots\ldots\ldots\ldots N-1.$$

If Y_k denotes the Fourier Transform of another time series y_n then the raw, unsmoothed crosspower estimate between x_n and y_n is given by -

$$P_{xy}(k) = X_k^* Y_k \tag{33}$$

where the asterisk denotes the complex conjugate. From Wiener-Khintchine theorem, the cross covariance function is -

$$C_{xy}(\tau) = \frac{1}{N} \sum_{k=0}^{N-1} P_{xy} e^{+\frac{2\pi i k\tau}{N}} \quad . \tag{34}$$

The covariances are next multiplied by the Parzen lag window, defined below, which has proven successful in obtaining smoothed and hence more stable spectra of the geomagnetic depth sounding records

$$\begin{aligned} W(\tau) &= 1 - 6\left(\frac{\tau}{M}\right)^2 + 6\left(\frac{\tau}{M}\right)^3 && |\tau| \leq \frac{M}{2} \\ &= 2\left(1-\left(\frac{\tau}{M}\right)\right)^3 && \frac{M}{2} < |\tau| \leq M \\ &= 0 && |\tau| > M \quad . \end{aligned} \tag{35}$$

Here, M is the half width of the Parzen lag window. Then the smoothed crosspower is given by

$$P_{xy}(k) = \sum_{\tau=-(M-1)}^{M-1} C_{xy}(\tau)\, W(|\tau|)\, e^{-\frac{2\pi i k\tau}{M}}. \tag{36}$$

Since $C_{xy}(-\tau) = C_{yx}(\tau)$ we can write -

$$P_{xy}(k) = \sum_{\tau=1}^{M-1} ((C_{xy}(\tau) + C_{yx}(\tau)) \text{ Cos } h - i\,(C_{xy}(\tau) - C_{yx}(\tau)) \text{ sin } h)\, W(|\tau|) + C_{xy}(o) \tag{37}$$

and the smoothed autopower is obtained by setting y=x i.e.

$$P_{xx}(k) = 2 \sum_{\tau-1}^{M-1} C_{xx}(|\tau|)\, W(|\tau|) \text{ Cos } h + C_{xx}(o), \tag{38}$$

where $h = \frac{2\pi k\tau}{M}$. (39)

The inverse Fourier Transform of equation (35) gives the spectral window defined as below -

$$W(w_j) = \frac{3M}{4} \left(\frac{\sin\,(w_j M/4)}{(w_j M/4)}\right)^4 \quad ; j = 0, 1, \ldots\ldots N-1 \tag{40}$$

$$w_j = \frac{2\pi j}{N}.$$

As noted by Jenkins and Watts (1968) the multiplication of the covariances by the lag window results in convolving the power spectrum with the spectral window $W(w_j)$. The process reduces the covariances by a factor R given by

$$R = \frac{1}{N}\int_{-M}^{M} W^2(\tau)d\tau = 0.54\frac{M}{N}. \tag{41}$$

The number of degrees of freedom when the Parzen window is used to smooth the spectra, is given by

$$\nu = \frac{2}{R} \simeq 3.71\ \frac{N}{M}. \tag{42}$$

The band width 'b' of the spectral window is given by

$$b = \frac{\nu}{2N} = \frac{1.86}{M}. \tag{43}$$

A reduction in the value of M results in an increase of the degree of freedom and also of the band width of the spectral window. This also results in smoothing over a wide range of frequencies and may distort the true spectral estimate.

It was mentioned earlier that when K events are averaged to obtain transfer functions $z_H(f)$ and $z_D(f)$, $\nu = 2(K-2)$. Thus, the total number of degrees of freedom, when spectra are smoothed by the Parzen window, is given by the product of ν with equation (42) i.e.

$$\nu = 3.71\ \frac{N}{M}\ (K-2). \tag{44}$$

One half the product is taken since the factor 2 has already appeared in equation (42). In equation (44) -

N = Number of data points in each time series including the number of zeros added to the end.

K = Number of isolated events used in obtaining the transfer functions

M = Half-width of the Parzen lag window.

Furthermore, to be significant the coherence should be greater than-

$$C_o(f) > \left(\frac{4}{v}\right)^{1/2} \quad \text{i.e. } C_o(f) > \left(\frac{1.08\ M}{(K-2)N}\right)^{1/2}$$

and the residual error should be less than the following -

$$E_o(f) < \left(1 - \frac{1.08\ M}{(K-2)N}\right)^{1/2} \quad .$$

The amplitudes and angles (azimuths) of the real and quadrature parts obtained by equations (24) and (25), at specific frequencies, are then averaged over a range of adjacent frequencies on the assumption that the transfer function varies slowly from estimate to estimate. Next, they are averaged at specific frequencies (periods) over all the available data records.

Table 1

Description of the IMS stations analysed in this study.

Station No.	Station Name	Code	Geographic Coordinates		Geomagnetic Coordinates*		Declination (°)
			Lat.(°N)	Long.(°W)	Lat.(°N)	Long.(°E)	
1	IGLOOLIK	IGL	69.4	81.8	77.4	353.9	-48.0
2	PELLY BAY	PEB	68.5	89.8	76.6	340.6	-27.5
3	RANKIN INLET	RIT	62.6	91.9	70.9	337.8	-5.0
4	ESKIMO POINT	EKP	61.1	94.1	69.2	335.3	2.0
5	FORT CHURCHILL	FCC	58.8	94.1	66.9	335.5	0.0
6	BACK	BKC	57.7	94.2	65.8	335.7	2.9
7	GILLAM	GIM	56.4	94.7	64.5	335.1	3.3
8	FORT SEVERN	FSV	56.0	87.6	64.4	344.2	-8.0
9	THOMPSON	TMP	55.7	97.9	63.8	331.0	9.8
10	ISLAND LAKE	ISL	53.9	94.7	62.1	335.4	3.8

*WALLIS and HUGHES (1982).

Table 2

Influence of Varying Parameters of the Conductor of the Selected Model (see Figure 6)

CONDUCTOR	PERIOD = 2.5 MIN. REAL TF	PERIOD = 2.5 MIN. QUAD. TF	PERIOD = 20 MIN. REAL TF	PERIOD = 20 MIN. QUAD. TF
Top at the surface	A	A	A	A
Top 5 km deep	A	A	A	A
Displaced 16 km to north (both cases above)	C	C+	C	C
8 km narrower	A+	A+	B+	A+
8 km wider	C	A	A+	B
extending deeper (94 km)	A-	A	B-	B
shallower (14 km)	A	B-	B-	A-
Resistivity = 50 ohm.m	B+	C+	C+	A-
Resistivity = 10 ohm.m	C	B+	A	B-
R=15 ohm.m below 10 km	A	B+	A-	B+
Same, but also 8 km narrower	A+	A	A-	A-
Dipping towards lower latitudes	B	B+	A-	A
Vertical	C	C	C	C

REFERENCES

Alabi, A.O., P.A. Camfield and D.I. Gough; The North American Central Plains Conductivity Anomaly, Geophys, J.R. astr. Soc. 43, 815-833, 1975.

Bailey, R.C., R.N. Edwards, G.D. Garland, R. Kurtz and D. Pitcher; Electrical Conductivity Studies over a tectonically active area in Eastern Canada; J. Geomeg. Geoelctr. 26, 125-146, 1974.

Banks, R.J.; Data processing and interpretation in geomagnetic deep sounding; Phys. Earth Planet. Liter. 7, 339-348, 1973.

Bendat, J.S. and Piersol, A.G.; Measurement and analysis of random data: John Wiley and Sons Inc., New York, p. 300, 1966.

Camfield, P.A., and Gough, D.I.; A possible Proterzoic plate boundary in North America, Can. J. of Earth Sciences, 14, 1229-1238, 1977.

Cooley, J.W. and Tukey J.W.; An algorithum for the machine computation of Complex Fourier Series; Mathematics of Computation 19, 297-307, 1965.

de Beer, J.H., J.S.V. van Zijl, and D.I. Gough; The southern cape conductive belt (South Africa): its composition, origin and tectonic significance; Tectonophysics, 83, 205-225, 1982.

Edwards, R.N., L.K. Law and A. White, Geomagnetic variations in the British Isles and their relation to electrical currents in the ocean and shallow seas; Phil. Trans. Roy. Soc. London A270, 289-323, 1971.

Gold, B. and C.M. Rader, Digital processing of signals, McGraw-Hill Book Co., Toronto, 1969.

Green, A.G., Z. Hajnal and W. Weber; Evolution of the Churchill Province and western margin of the Superior Province in Canada and the North-Central United States, to be submitted 1983.

Handa S. and P.A. Camfield; crustal electrical conductivity in North-Central Saskatchewan: The North American Central Plains Anomaly and its relation to a Proterzoic Plate Margin, Can. J. Earth Sciences, (submitted 1983).

Innes, M.J.S., Gibb, R.A., Hall, D.H. and A.S. MacLaren; Geophysical characters and deep structure of the Superior province. In Price, R.A. and Douglas, R.J.W. 1972, Variations in tectonic styles in Canada. Geological Association of Canada, special paper 11, 589-603, 1972.

Jenkins, G.M. and D.G. Watts; Spectral Analysis and its Applications, Holden Day Inc. San Francisco, 1968.

Ku, C.C., M.S. Hsieh, and S.H. Lim; The topographic effect in electromagnetic fields, Can. J. Earth Sci. 10, 645-656, 1973.

Lewry, J.F., Stauffer M.R., and S. Fumerton; A cordilleran-type batholithic belt in the Churchill Province in northern Saskatchewan, Precambrian Research 14, 277-313, 1981.

Lewry, J.F., Lower Proterzoic Arc-Microcontinent collisional techonics in the western Churchill Province, Nature 294, 69-72, 1981.

Loomer, E.I. and J.C. Gupta; Some characteristics of high latitude substorms, J. Atmos. Terr. Phys. 42, 645-652, 1980.

Parkinson, W.D.; Direction of rapid geomagnetic fluctuations, Geophys. J.R astr Soc. 2, 1-14, 1959.

Parkinson, W.D.; The influence of Continents and Oceans on geomagnetic variations; Geophys. J.R. astr. Soc. 4, 441-449, 1962.

Parkinson, W.D., Conductivity anomalies in Australia and ocean effect, J. Geomagn. Geoelectr. 15, 222-226, 1964.

Plet F.C. and G. Jansen van Beek; Data aquisition for the International magnetospheric study at the Churchill Array of magnetic variometer stations; Earth Physics Branch Open File No. 82-4, 1982.

Schmucker, U.; Anomalies of geomagnetic variations in the south-western United States, Scipps Institution of Oceanography Bulletin, 13, 165 pp, 1970.

Strangway, D.W., Redman, J.D. and Macklin, D; Shallow electrical sounding in the precambrian crust of Canada and the United States, in the Continental Crust and its Mineral Deposits, edited by D.W. Strangway, Geological Association of Canada, Special Paper, 20, 273-301, 1980.

Wallis D.D., and T.J. Hughes; Magnetic Coordinates of High Latitude North American Population Centers, National Research Council of Canada, Ottawa, Canada. Internal Publication 1982.

FIGURE CAPTIONS

Fig. 1. Map of Canada showing the location of the stations from which IMS data are used for the present investigation.

Fig. 2a. Magnetograms of the geomagnetic H, D and Z - components during the IMS interval on May 6, 1977 (day 126), on May 11, 1977 (day 131), on August 27, 1979 (day 239) and on September 25, 1979 (day 268).

Fig. 2b. Simultaneous records on a larger scale than the one in Figure 2a for 6 hours on September 4, 1979 (day 247) from Eskimo Point (EKP), Back (BKC), Gillam (GIM), Fort Severn (FSV), Thompson (TMP) and Island Lake (ISL).

Fig. 2c. Magnetograms between 1700-1800 UT on September 4, 1979 prepared from 10s data from Back (BKC) and Gillam (GIM). A large phase shift may be noted easily in the vertical component variations. Such reversals are first indications of an induction anomaly between the stations.

Fig. 3. Azimuths and amplitudes of the real (in-phase) (O) and imaginary (quadrature-phase) (Δ) transfer functions. The error bars are one standard deviation about the mean values.

Fig. 4. The vertical-field response arrows giving the amplitude and direction of the transfer functions at all the nine stations at 8 different periods ranging from 2.5 min. to 162 minutes. The

in-phase arrows shown in the upper part of the diagram have been reversed to point towards the internal currents and away from the external currents. The quadrature-phase arrows are shown in the lower part of the diagram.

Fig. 5 Amplitude of the real and quadrature transfer functions projected on a north-south profile. Note the anomalous behaviour of the curves at the station FSV.

Fig. 6 In-phase and quadrature responses at 2.5 min and 20 min periods were computed for the two-dimensional conductivity structure shown in the upper right. The observed values of the transfer functions projected on a north-south line are shown by circles with error bars representing one standard deviation from the average values and the calculated values are shown by the solid curves.

Fig. 7 Tectonic units on the exposed Canadian Shield of Manitoba and Saskatchewan from Green et al. (1983). TB - Thompson belt; FRB - Fox River belt; KG - Kisseynew gneiss belt; FF-SL - Flin Flon-Snow Lake belt; HLB - Hanson Lake block; GL - Glennie Lake domain; LR-LL - La Ronge-Lynn Lake belt; R-SI - Reindeer-South Indian Lakes belt; W-C - Wathaman-Chipewyan batholith; PLC - Peter Lake complex; W - Wollaston domain; SR - Seal River domain; N - Nejanilini domain; M - Mudjatik domain; V - Virgin River domain; CLZ - Cree Lake zone

(includes the Wollaston, Seal River, Nejanilini, Mudjatik and Virgin River domains); CC - Churchill craton; TFF - Tabbernor fault/fold zone; S - Stanley Shear zone; NF - Needle Falls shear zone; PL - Parker Lake shear zone; VR - Virgin River shear zone; AB - Athabasca basin.

Fig. 8 Location of the North American central plains conductive body (broad shaded area). In the Churchill Province the Wathman-Chipewyan Batholith lies to the north and the bulk of the Kisseynew gneiss belt to the south of the conductor. The triangles locate the array of 41 magnetometers from Alabi et al. (1975) and the permanent observatory at Meanook (MNK), the crosses locate an array of 7 magnetometers established by Handa and Camfield (1983) and dots represent the IMS stations of the present study.


120°
60°
80°
BAFFIN I.
IGL
PEB
NORTHWEST
TERRITORIES
60°
RIT
EKP
HUDSON
BAY
FCC
BKC
ALBERTA
SASK.
TMP
GIM
FSV
ISL
QUEBEC
MAN.
ONTARIO
U.S.A.
40°
500 km

FIGURE 1

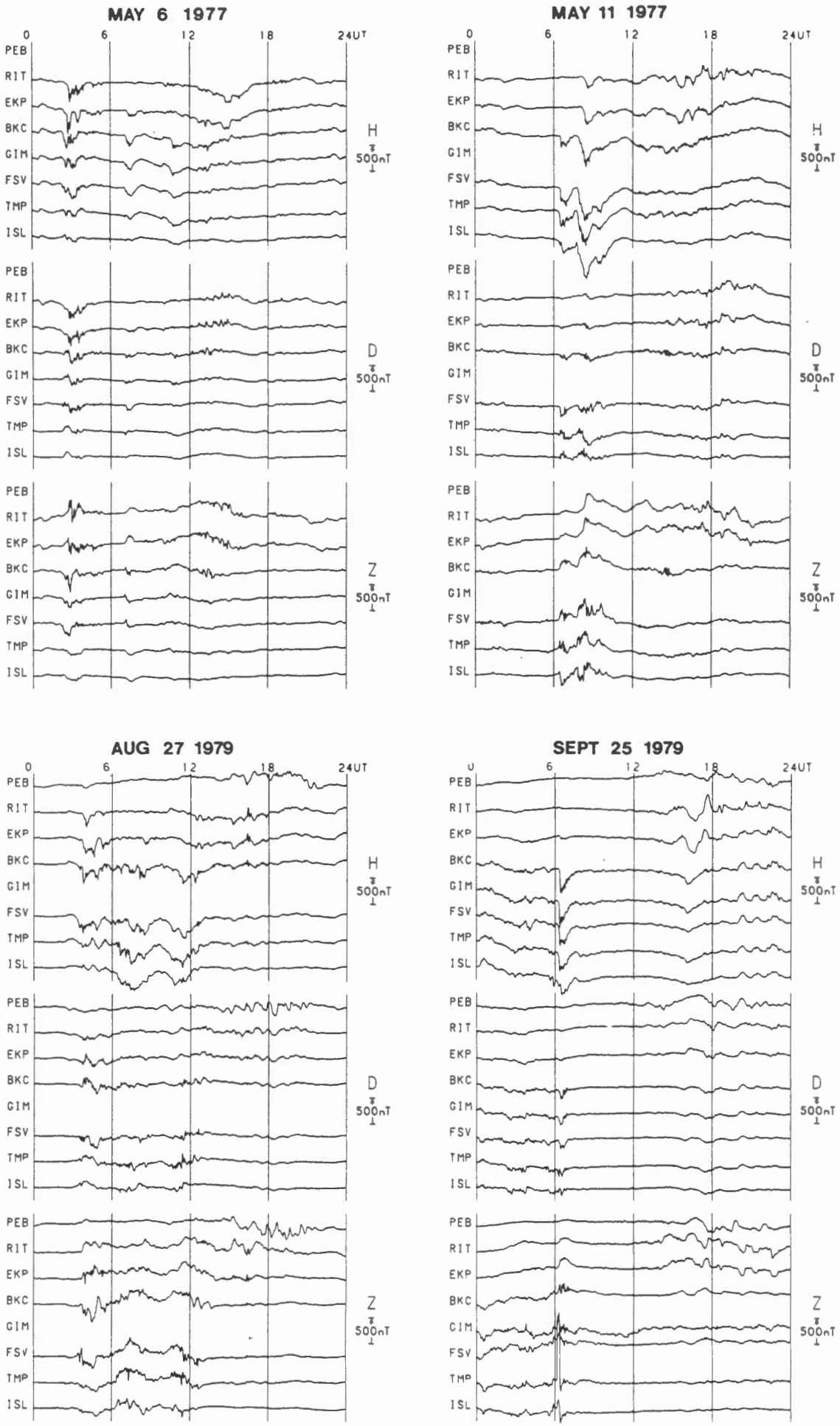
MAY 6 1977
MAY 11 1977
AUG 27 1979
SEPT 25 1979
0
6
12
18
24UT
PEB
RIT
EKP
BKC
GIM
FSV
TMP
ISL
H
D
Z
500nT

FIGURE 2a

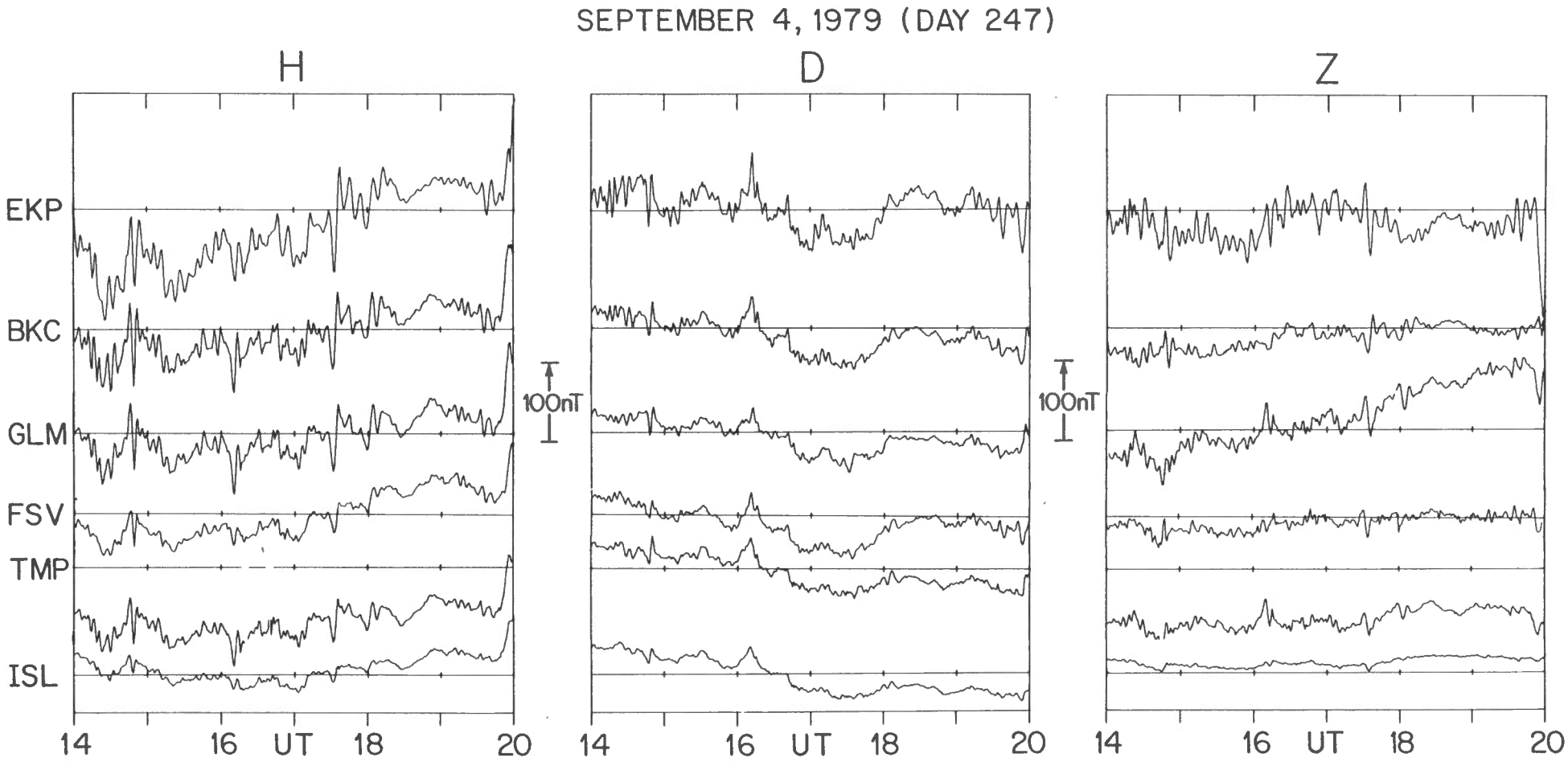
SEPTEMBER 4, 1979 (DAY 247)
H
D
Z
EKP
BKC
GLM
FSV
TMP
ISL
100nT
100nT
14
16
UT
18
20
14
16
UT
18
20
14
16
UT
18
20

FIGURE 2b

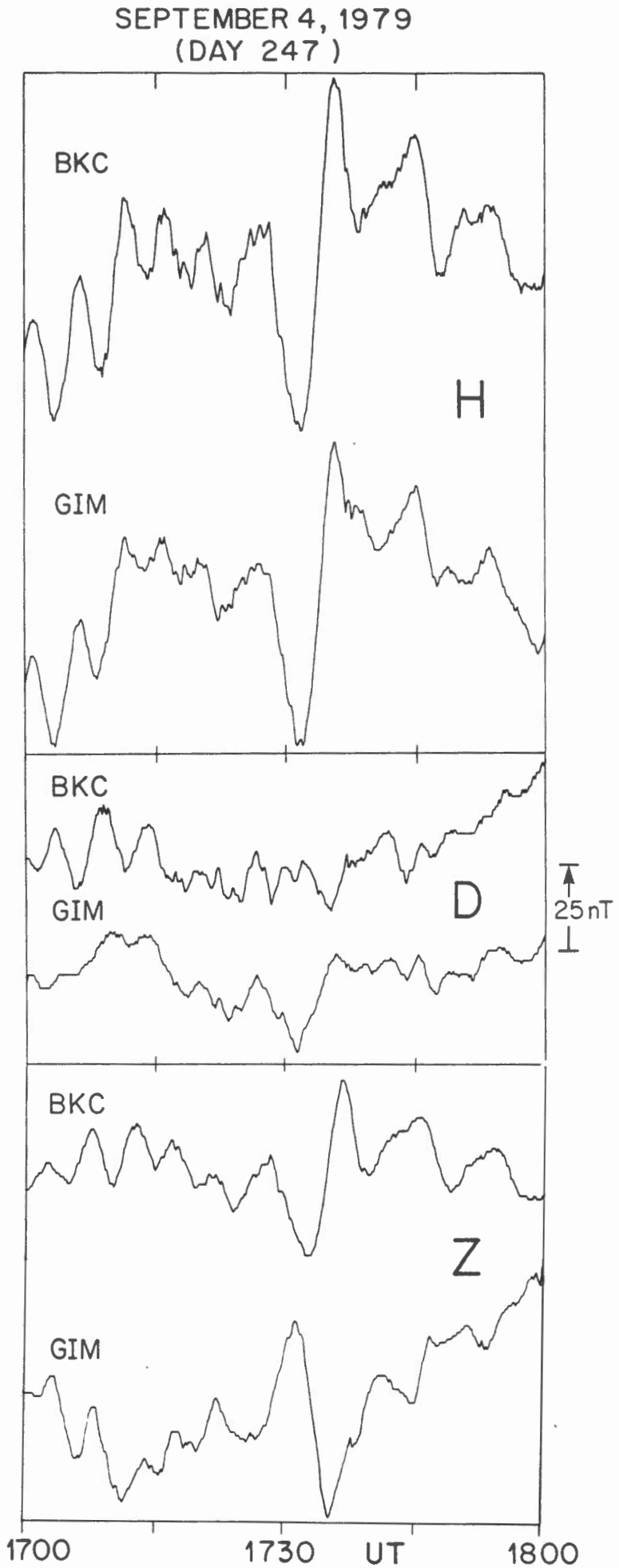
SEPTEMBER 4, 1979
(DAY 247)
BKC
H
GIM
BKC
D
GIM
25nT
BKC
Z
GIM
1700
1730
UT
1800

FIGURE 2c

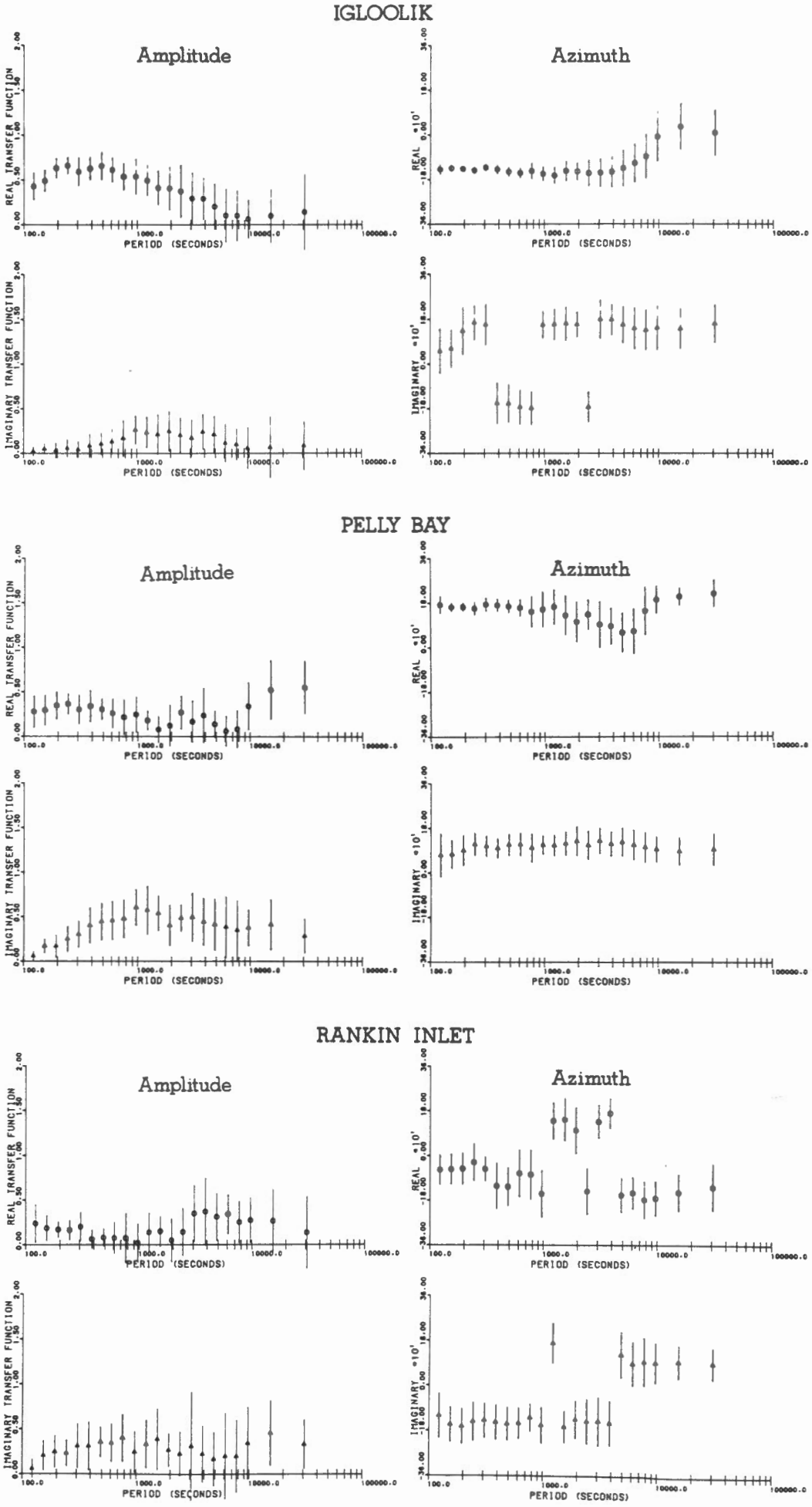
IGLOOLIK
Amplitude
Azimuth
REAL TRANSFER FUNCTION
IMAGINARY TRANSFER FUNCTION
REAL *10'
IMAGINARY *10'
PERIOD (SECONDS)
PELLY BAY
Amplitude
Azimuth
REAL TRANSFER FUNCTION
IMAGINARY TRANSFER FUNCTION
REAL *10'
IMAGINARY *10'
PERIOD (SECONDS)
RANKIN INLET
Amplitude
Azimuth
REAL TRANSFER FUNCTION
IMAGINARY TRANSFER FUNCTION
REAL *10'
IMAGINARY *10'
PERIOD (SECONDS)

FIGURE 3

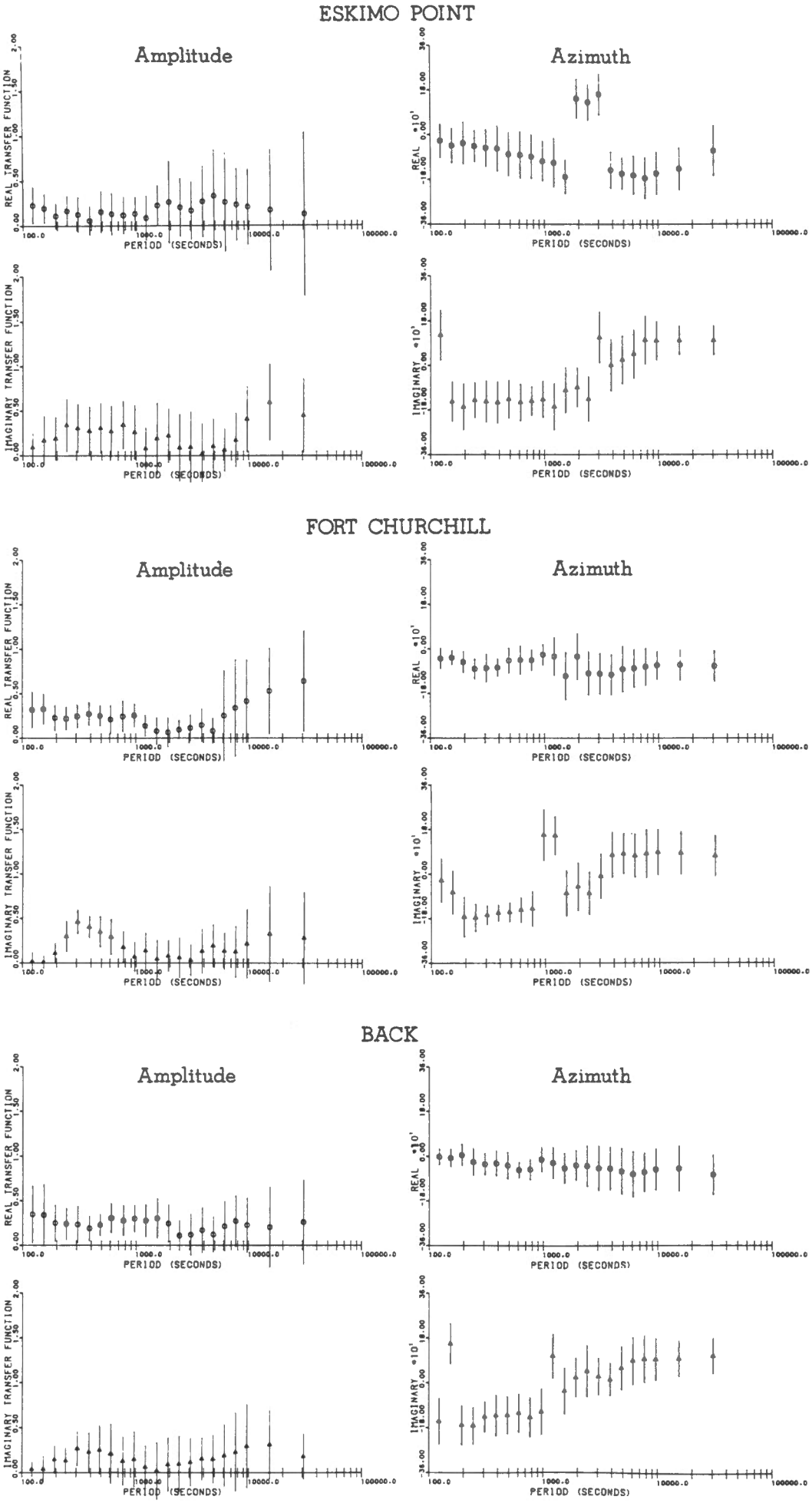

FIGURE 3(cont..)

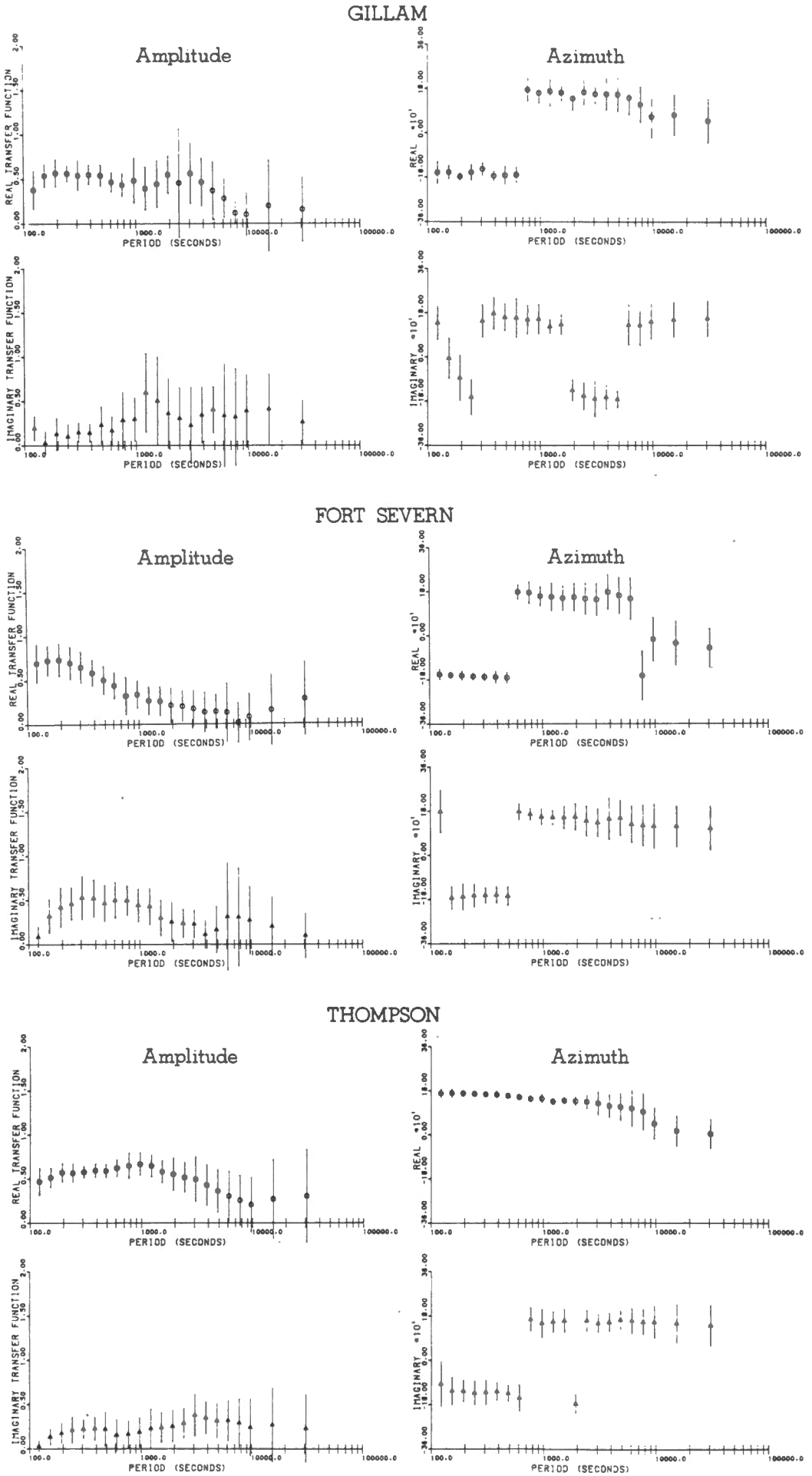

FIGURE 3(cont..)

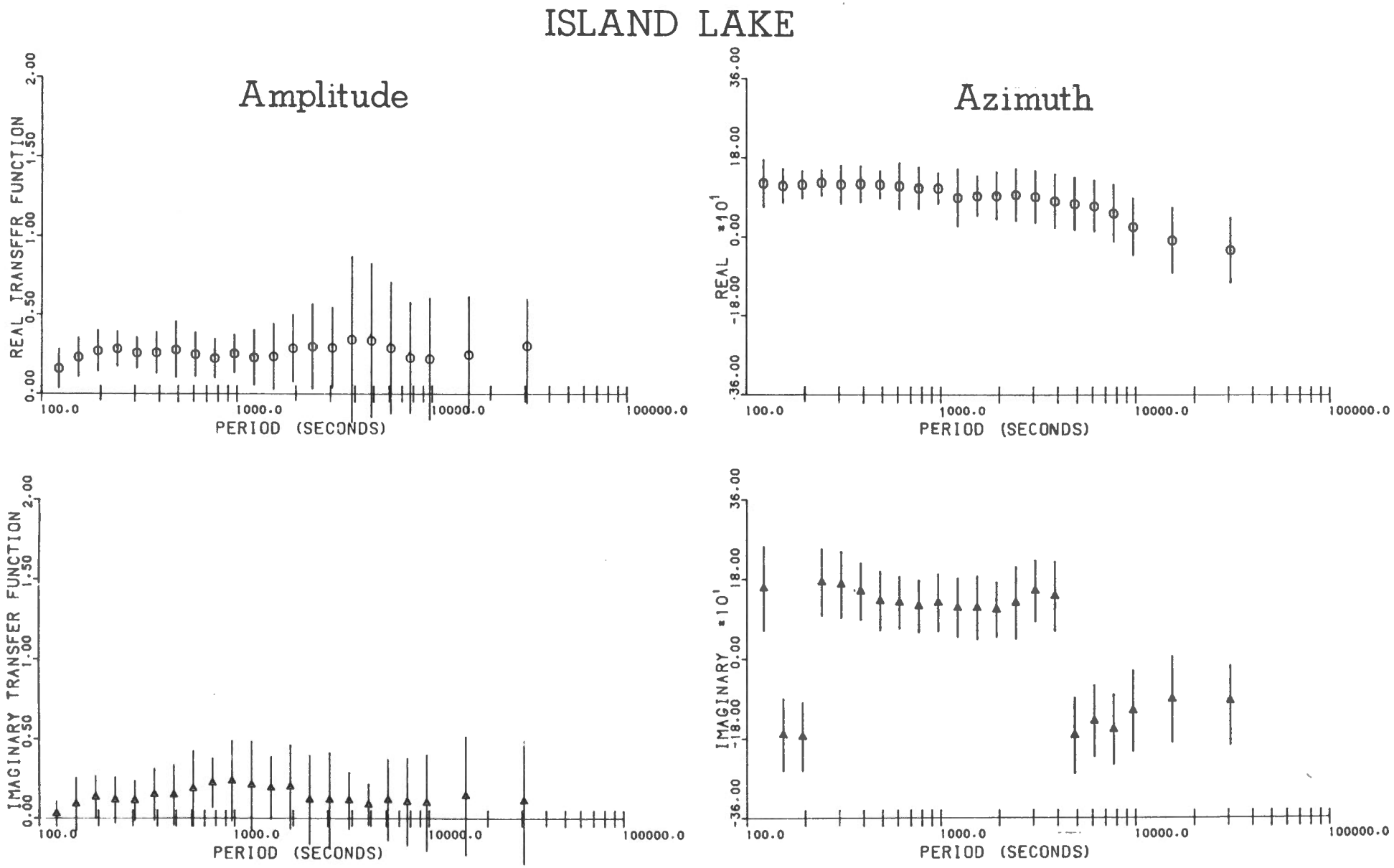

FIGURE 3(cont..)

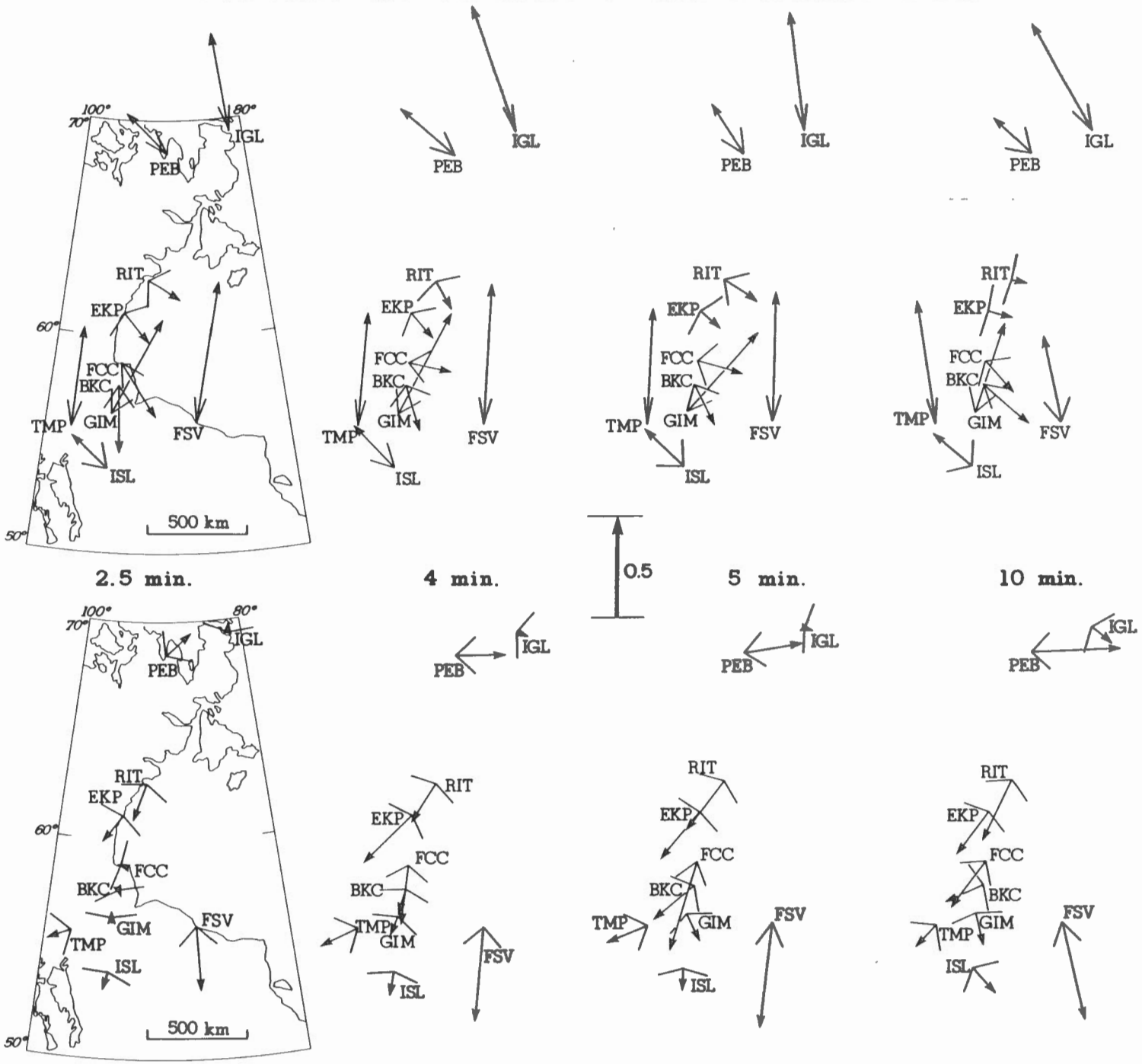
AMPLITUDE AND DIRECTION OF REAL TRANSFER FUNCTION
100°
80°
70°
60°
50°
IGL
PEB
RIT
EKP
FCC
BKC
TMP
GIM
FSV
ISL
500 km
0.5
2.5 min.
4 min.
5 min.
10 min.
AMPLITUDE AND DIRECTION OF QUADRATURE TRANSFER FUNCTION

FIGURE 4

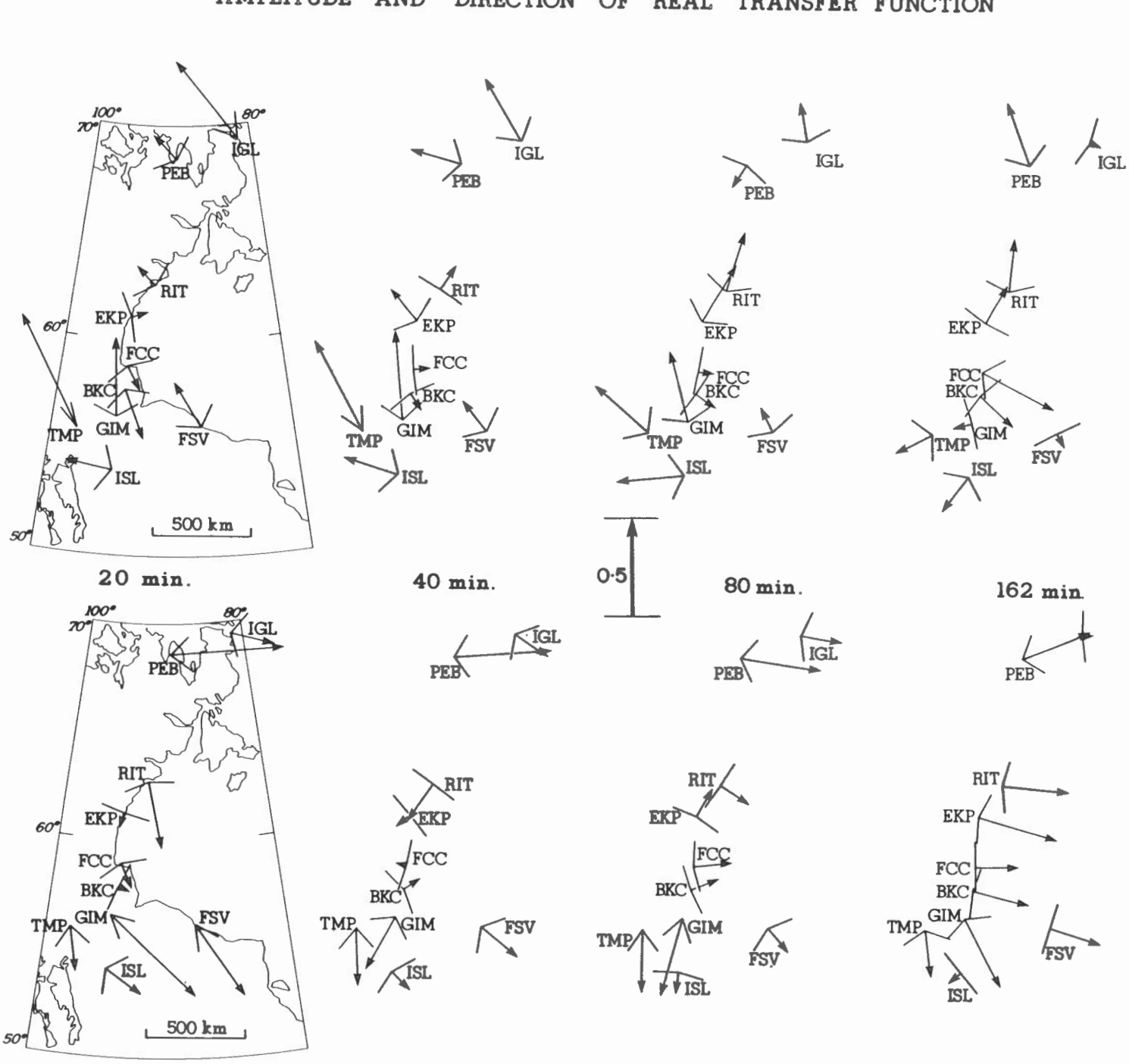

FIGURE 4(cont..)

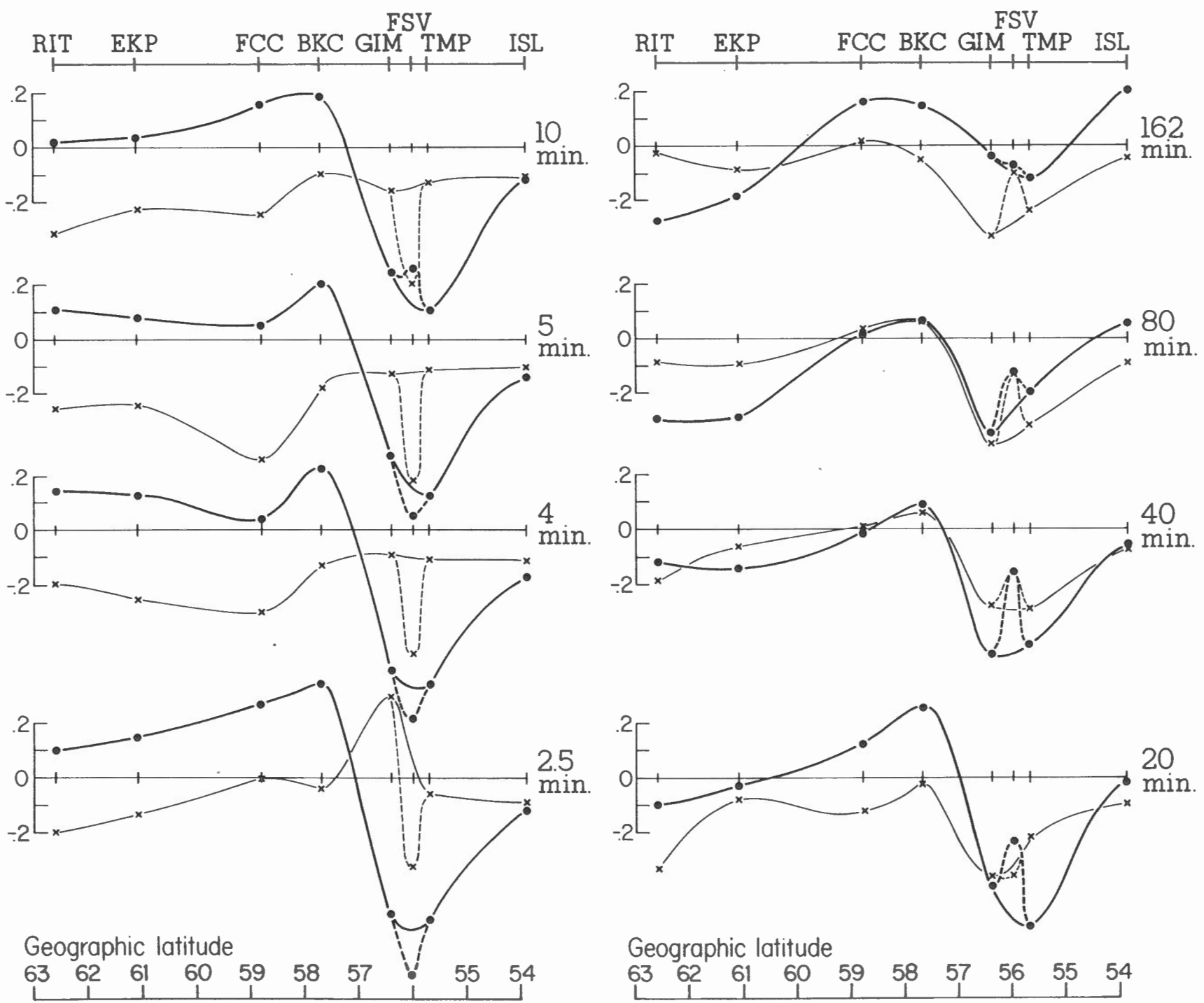
AMP OF THE NORTHERN COMPONENT OF
REAL TF
QUADRATURE TF
RIT
EKP
FCC
BKC
GIM
FSV
TMP
ISL
.2
0
-.2
10 min.
5 min.
4 min.
2.5 min.
162 min.
80 min.
40 min.
20 min.
Geographic latitude
63 62 61 60 59 58 57 55 54
63 62 61 60 59 58 57 56 55 54

FIGURE 5

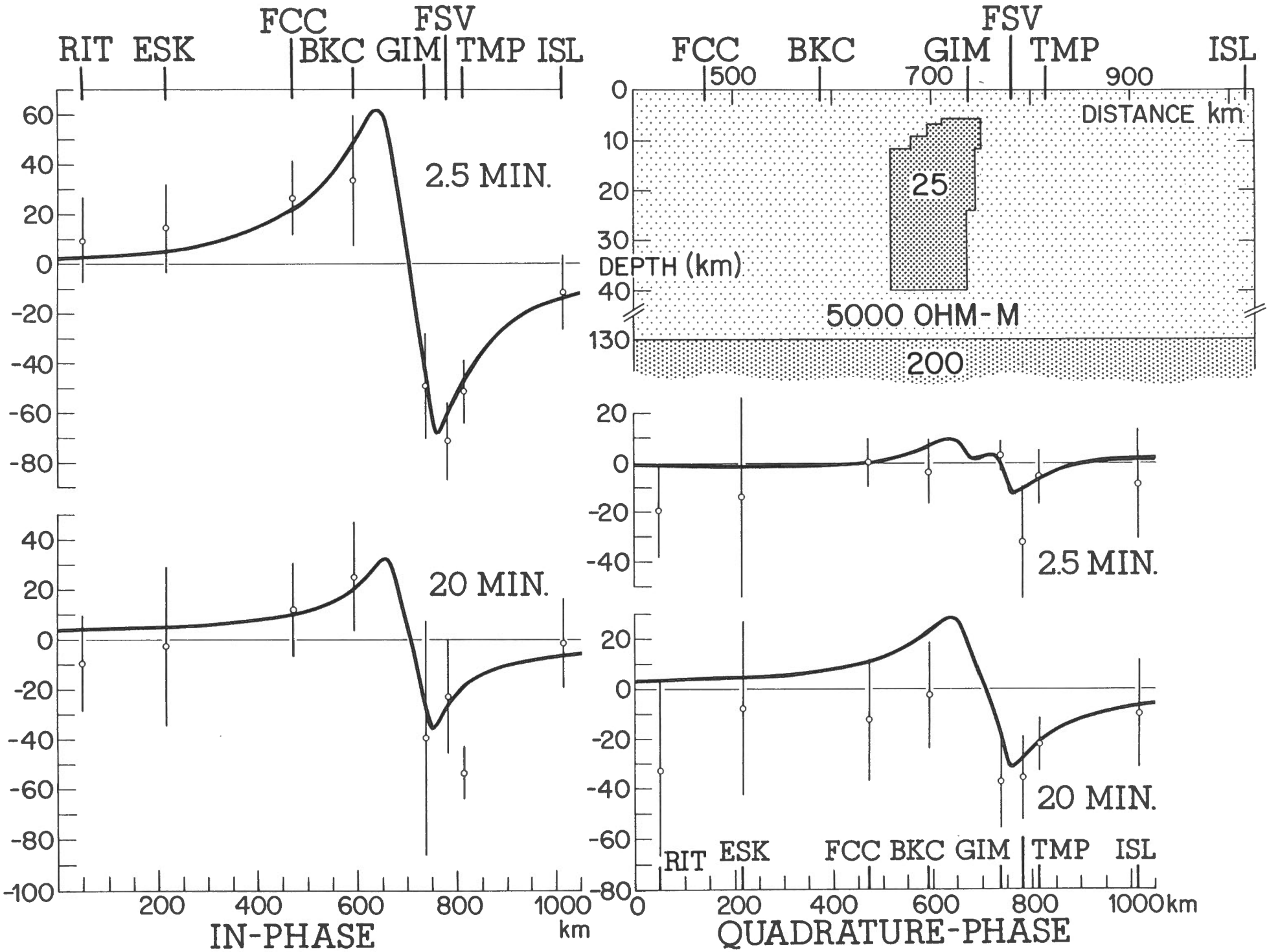
RIT
ESK
FCC
BKC
FSV
GIM
TMP
ISL
2.5 MIN.
20 MIN.
IN-PHASE
km
500
700
900
DISTANCE km
DEPTH (km)
25
5000 OHM-M
200
QUADRATURE-PHASE

FIGURE 6

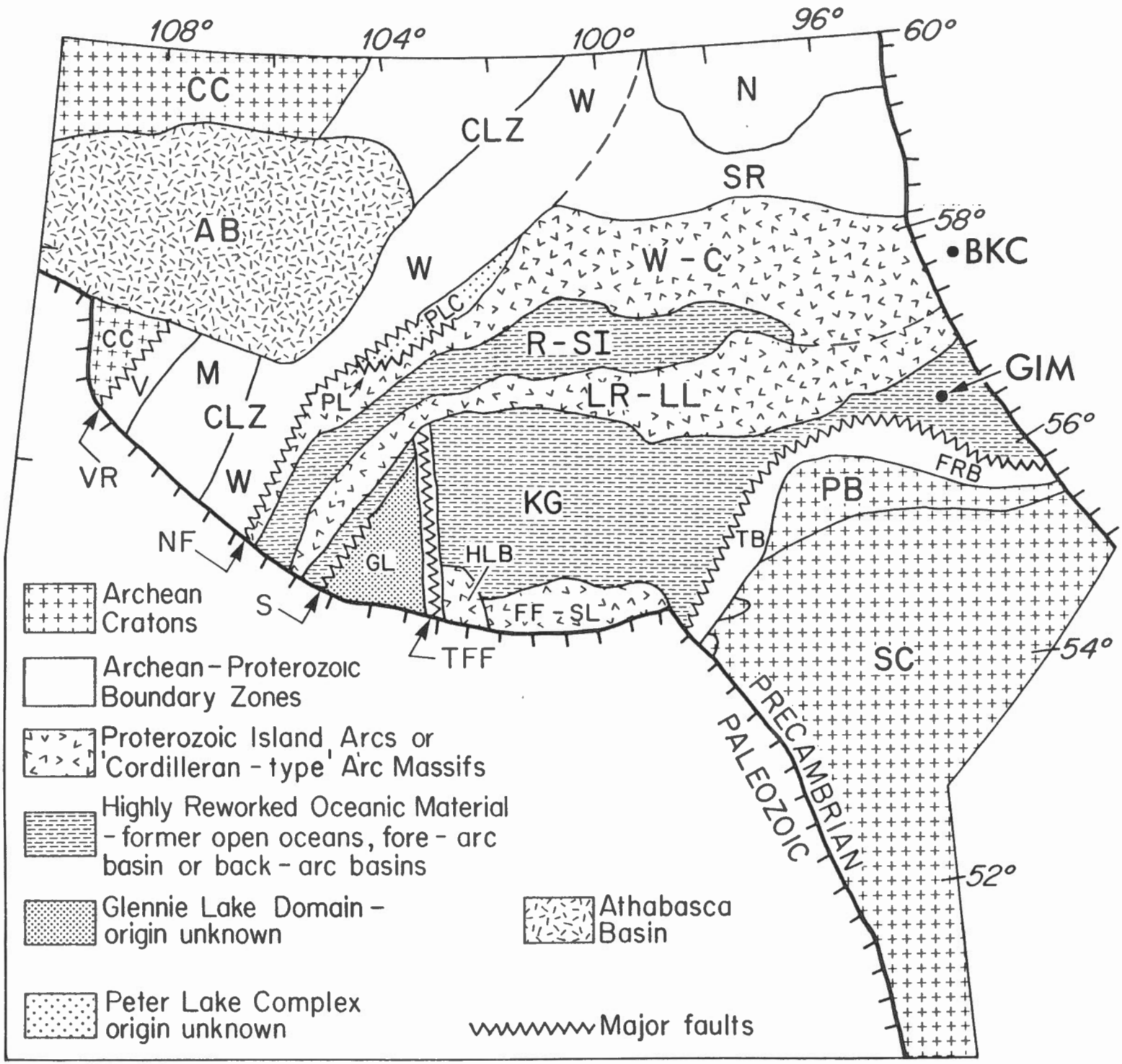
108°
104°
100°
96°
60°
58°
56°
54°
52°
CC
CLZ
W
N
SR
AB
W
W - C
BKC
PLC
R - SI
GIM
CC
M
CLZ
PL
LR - LL
VR
W
FRB
PB
KG
NF
GL
HLB
TB
S
FF - SL
TFF
SC
PRECAMBRIAN
PALEOZOIC
Archean Cratons
Archean - Proterozoic Boundary Zones
Proterozoic Island Arcs or 'Cordilleran - type' Arc Massifs
Highly Reworked Oceanic Material - former open oceans, fore - arc basin or back - arc basins
Glennie Lake Domain - origin unknown
Athabasca Basin
Peter Lake Complex origin unknown
Major faults

FIGURE 7


70°
120°
100°
80°
70°
500 km
60°
60°
HUDSON
BAY
CHURCHILL
PROVINCE
ALBERTA
BKC
GIM
GREAT PLAINS
MANITOBA
SUPERIOR PROVINCE
50°
50°
Saskatoon
Regina
SASK.
MONTANA
N. DAKOTA
WILLISTON
BASIN
S. DAKOTA
BLACK
HILLS
GREAT
PLAINS
WYOMING
BASIN
NEBRASKA
SOUTHERN
ROCKIES
DENVER
BASIN
40°
120°
110°
100°
90°
80°
40°

FIGURE 8